Photodissociation of the Formaldehyde Molecule: Does It or Doesn't It?

WILLIAM M. GELBART*

Department of Chemistry, University of California, Los Angeles, Los Angeles, California 90024

MARK L. ELERT

Department of Chemistry, U.S. Naval Academy, Annapolis, Maryland 21402

DONALD F. HELLER

Materials Research Center, Allied Chemical Corporation, Morristown, New Jersey 07960

Received July 16, 1979 (Revised Manuscript Received March 25, 1980)

Contents

After obtaining his B.S. (1967) and Ph.D. (1970) at Harvard and the University of Chicago, respectively, William Gelbart enjoyed a couple years of postdoctoral research at the University of Paris, Orsay, and the University of California, Berkeley. He then taught at Berkeley for 3 years before joining the UCLA faculty, where he is presently Professor of Chemistry and Camille and Henry Dreyfus Teacher–Scholar. His research interests include liquid-crystal phase transitions, light scattering from condensed states of matter, and intramolecular electronic and vibrational relaxation.

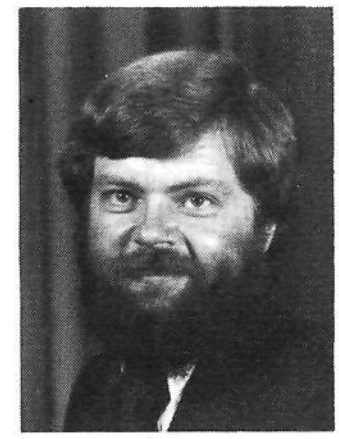

Mark Elert received his B.S. degree in chemical physics from Michigan State University and did his graduate work with Professor William Gelbart at UC Berkeley. After obtaining his Ph.D. in 1977, he taught at UCLA for two years before moving to his present position as assistant professor of chemistry at the U.S. Naval Academy.

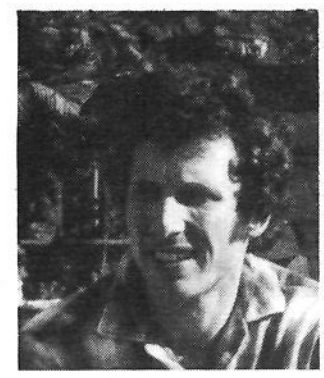

Donald Heller has been a staff chemical physicist at Allied Chemical Corporation's Material Research Center since 1977. His recent theoretical and experimental interests include the chemical dynamics of highly vibrationally excited polyatomic molecules, multiphoton processes, and molecular overtone spectroscopy.

I. Introduction

The considerable conceptual and practical difficulties associated with the photodissociation dynamics of polyatomic molecules have been reviewed several times in the recent literature.[1] As stressed there, the situation for polyatomics is tremendously more complicated than that for diatomics—this is, of course, because there is more than one vibrational degree of freedom. Knowing that the total energy lies above the dissociation threshold does not allow us to conclude that the excited molecule will break up on an observable time scale. Nor do we know a priori what the reaction coordinate will be and how it will exchange energy with the electrons and remaining vibrational modes. As a result, there is not a single polyatomic molecule (including collinear triatomics) for which the actual "mechanism" of photodissociation is unambiguously established, i.e., where we know which electronic states are involved and how the nuclear motions are coupled.

The one polyatomic molecule which has probably been studied more thoroughly than any other—from the point of view of fragmentation dynamics—is formaldehyde (H_2CO). Following optical excitation to low-lying rotational–vibrational levels of the first excited singlet state, formaldehyde is known to dissociate to H_2 + CO and/or H + HCO (depending on the excitation wavelength). A wealth of information is available concerning properties of the formaldehyde molecule in all of the electronic states accessible at the energies of interest, and a great deal of kinetic data on the dissociation process has also been reported.

On the theoretical side, first Morokuma et al.[2] and then van Dijk et al.[3] and Goddard and Schaefer[4] have generated SCF–CI

0009-2665/80/0780-0403$05.00/0

potential-energy surfaces for the ground (S_0, $^1A_1$), first triplet (T_1, $^3A_2$), and first excited singlet (S_1,$^1A_2$) electronic states. Ab initio calculations for these lowest lying configurations had been carried out earlier by several groups, at special (e.g., equilibrium) nuclear geometries.[5-7] There are also many theoretical treatments[8-11] of the Herzberg–Teller (vibronic) coupling in formaldehyde, in which approximations are suggested for the nuclear-coordinate dependence of the electronic wave functions for these states. van Dijk et al.[12] have specifically avoided the Herzberg–Teller expansion and have calculated nonadiabatic interactions by assuming instead a separability for their nuclear-coordinate dependence.

On the experimental side, a large amount of low-pressure spectroscopic and kinetic data is available. High-resolution electronic ($S_0 \rightarrow S_1$, T_1) spectra have been analyzed by Innes et al.[13] and by Jones and Coon,[14] with S_1–T_1 perturbations studied in particular by Brand et al.[15] and by Birss, Ramsay, and Till.[16] (See ref 17 for a comprehensive review of the ultraviolet spectroscopy of formaldehyde.) Quantum yields for the formation of atomic and molecular hydrogen[18-21] as well as HCO reaction rates[22] have been measured following the photolysis of parent H_2CO. In addition, the lowest triplet state (T_1) has been implicated[23-25] in the formaldehyde decomposition, as has the ground state (S_0) hydroxymethylene isomer.[26] Finally, Moore and co-workers,[27-31] Lee and co-workers,[32-35] Selzle and Schlag,[36] and Luntz[37] have obtained extensive data on the low-pressure lifetimes and fluorescence quantum yields associated with rotational–vibrational features of S_1 and have time resolved the appearance of fragments following optical excitation of S_1. Finally, formaldehyde has been chosen by Troe and co-workers[38] as a focal point for their collisional studies of unimolecular reactions; many new data are now becoming available on the shock-tube (1500 K < T < 2400 K) characteristics of the dissociations to H_2 + CO and H + HCO.

Some of the many questions which arise from the above experiments are the following: (1) Do the barriers against dissociation lie above or below the S_1 excitation energy? (2) Is the nonradiative process by which S_1 decays at low pressure collision induced? (3) Or is it induced by tunneling on the S_0 surface? (4) Does it involve coupling with T_1, or only with S_0? (5) Does formaldehyde, excited optically near the S_1 origin, dissociate in the absence of collisions? (6) Do H and HCO radicals play an important role in the formation of molecular products? (7) Once H_2CO reaches the ground-state (S_0) potential-energy surface, does it dissociate immediately, or is there a time lag associated with the intramolecular vibrational energy redistribution and rearrangement necessary for reaction? (8) Or is the time lag associated with thermal activation over the barrier? (9) Or with collision-induced vibrational energy redistribution? (10) What is the origin of the dramatic dependence observed on rotational quantum number of the optically prepared S_1 level?

The answers to the above questions constitute nothing more or less than the "mechanism" of the formaldehyde photodissociation dynamics. In this communication we emphasize just how much is *not* understood about this important example. In the next section (II) we present the key experimental facts which set the scene for possible interpretations of the formaldehyde photodissociation dynamics. These data pose more precisely the conceptual questions which were raised out of context in the above paragraph. The amount of detail available from these several state-of-the-art experiments is staggering, and yet we will find that little of the photodissociation "mechanism" is resolved by them.

In section III we outline briefly two recent theoretical approaches to the problem. First (IIIA) we describe the basic coupling scheme and damping matrix (effective Hamiltonian) formalism of Elert, Heller, and Gelbart[39,40] and present some

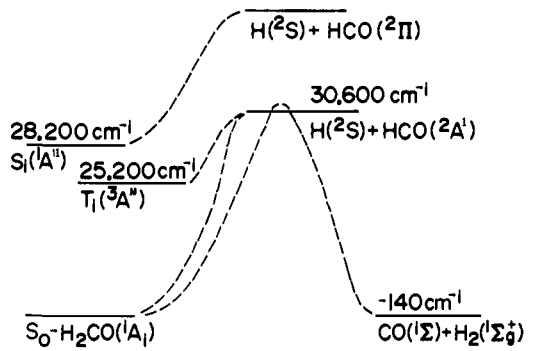

Figure 1. Schematic diagram showing energies of, and correlations between, the low-lying electronic states of H_2CO and its fragments.

results of their numerical computations. These are compared and contrasted in IIIB with the alternative methods employed by van Dijk, Kemper, and Buck.[12,41,42] Then, in section IV, we consider the effects of neglect of rotation and T_1 effects and of many other simplifying approximations invoked in the theoretical analyses. We resurrect the possibility of tunneling (through the S_0 barrier), which process had been excluded in the original numerical computations. This possibility is argued to provide the most likely explanation of the collisionless nonradiative decay observed for the low-lying rotational–vibrational levels of S_1. But tunneling, as well as the less-likely explanations, cannot account for the higher pressure "time lag" measured for the appearance of CO products. Accordingly, it has proved necessary to assert the existence of a "long-lived" intermediate which is formed from S_1 by collision and which cannot dissociate without further collision. We offer detailed criticism of the various species which have been proposed as candidates for the intermediate and conclude with a summary of the few features which have been established beyond any reasonable doubt and with a list of yet-to-be-solved theoretical questions and yet-to-be-tried experimental studies.

II. Experimental Background

A. General Considerations

Figure 1 shows a schematic energy level diagram for the low-lying states of H_2CO and its radical and diatomic products. Only the ground electronic (S_0) state of H_2CO correlates with ground electronic states of H_2 + CO. This reaction is essentially thermoneutral, but there is a huge barrier to products along the minimum energy pathway. The consensus from the most recent ab initio calculations[4] is that the S_0 barrier (henceforth referred to as D) does not lie lower than $\sim$32 000 cm^{-1}. S_0 also correlates with the ground electronic states of H + HCO, as does T_1. Measured[18,20,21] photochemical thresholds for the $H_2CO \rightarrow H(^2S) + HCO(^2A')$ reaction suggest a value of $\sim$30 600 cm^{-1} in agreement with earlier thermodynamic estimates.[43] Thus, if we confine our attention to optical excitation of H_2CO near enough the S_1 origin [e.g., the zero-point (28 188 cm^{-1}) vibrational band], we need not worry about the possibility of radical formation.

Let us proceed, then, by considering only the ground and first excited singlet state near the S_1 origin. The equilibrium nuclear geometries are well established for both states, from microwave studies of S_0[44] and vibrational–rotational analysis[14] of the S_0–S_1 ultraviolet absorption. The principal changes in geometry, upon excitation, involve the CH_2 group coming 34° out of the molecular plane and the CO bond length increasing by 10% (see Table IA). These two modes also undergo among the largest S_0–S_1 frequency changes (see Table IIA). The CH_2 out-of-plane "wag" and CO stretch are thus the strongly excited modes in

Table I. Geometry and Coordinate Systems for Formaldehyde[a]

A. Cartesian Axes and Internal Coordinates

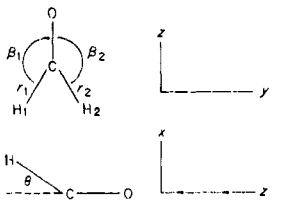

	$^1A_1$ (S_0)	$^1A''$ (S_1)
R	1.208 Å	1.325 Å
r	1.116 Å	1.095 Å
β	121.75°	121.0°
θ	0°	33.6°

B. Symmetry Coordinates

	definition	description
S_1	$(1/2^{1/2})(\delta r + \delta r_2)$	symmetric C-H stretch
S_2	δR	C-O stretch
S_3	$(1/2^{1/2})(\delta\beta_1 + \delta\beta_2)$	symmetric H-C-H bend
S_4	$\delta\theta$	out-of-plane bend
S_5	$(1/2^{1/2})(\delta r_1 - \delta r_2)$	asymmetric C-H stretch
S_6	$(1/2^{1/2})(\delta\beta_1 - \delta\beta_2)$	asymmetric H-C-H bend

[a] (A) R, r, and β denote the CO bond length, CH bond lengths, and HCO angles, respectively; θ is the out-of-plane "wag" angle. At the equilibrium configuration, symmetry requires $r_1 = r_2 = r$ and $\beta_1 = \beta_2 = \beta$. (B) "Plus" and "minus" combinations of the CH stretch displacements (δr_1, δr_2) and of the CHO bend displacements ($\delta\beta_1$, $\delta\beta_2$) comprise the first, fifth, third, and sixth symmetry coordinates; δR and $\delta\theta$ correspond directly to the remaining second and fourth.

the S_0–S_1 vibrational progressions.

B. S_1 (Zero-Point) Lifetimes

The road to good zero-pressure fluorescence lifetimes for individual ro-vibrational levels of S_1 has been a long and rocky one; it is reviewed in several recent articles.[30,31,34,45]

For our present purposes it suffices to discuss only the most recent data of Weisshaar and Moore.[31] Using the nitrogen laser pumped dye laser (with fwhm of $\sim$0.15 cm^{-1}) they succeeded in selectively exciting over 100 rotational levels belonging to the S_1 origin (zero-point vibrational level). In over 90% of these cases the time-resolved fluorescence was observed to be simple exponential. At low pressures ($\lesssim$1 torr) the Stern–Volmer plots, i.e., plots of fluorescence rate ($1/\tau_{S_1}$) vs. pressure (P), are in general highly nonlinear. But in the lowest pressure range (0.5–10 mtorr) they become linear, with slopes (quenching rates) typically on the order of 10^8 s^{-1}/torr ($\sim$10 times the gas kinetic rate). Thus a reasonably unambiguous extrapolation of τ_{S_1} to zero pressure was possible.

The zero-pressure S_1 fluorescence lifetimes obtained by Weisshaar and Moore were found to vary from 66 to 4170 ns. τ_{S_1}'s longer than 500 ns or shorter than 100 ns were unusual, the typical being $\sim$150 ns. (These data agree with the several zero-point rotational lifetimes measured by Luntz[37] in his effusive molecular beam apparatus; the lifetimes reported by Selzle and Schlag[36] from their supersonic jet studies refer to higher lying vibrational states.) Within the zero-point vibrational band, the variation of τ_{S_1} with rotational level was seen to be strong (factor of 60!) and essentially random. This explains immediately why the earlier τ_{S_1} measurements were discrepant with one another. In the earlier experiments whole bunches of rotational levels were excited at a time, thus leading to multiexponential fluorescence decays with a broad distribution of lifetimes. Furthermore, few of the earlier measurements had been carried out at low enough pressures for the Stern–Volmer plots to become linear. Thus the extrapolations to zero-pressure fluorescence rates were often made with incorrect slopes.

Table II

A. Normal Modes of Vibration for Formaldehyde[a]

mode	sym-metry (C_{2v})	H_2CO frequency, cm^{-1}		D_2CO frequency, cm^{-1}	
		$^1A_1$	$^1A_2$	$^1A_1$	$^1A_2$
1	A_1	2766.4	2847.0	2055.8	2079.0
2	A_1	1746.1	1173.0	1700.0	1176.0
3	A_1	1500.6	887.0	1105.7	(625)
4	B_1	1167.3	689.4[b]	933.8	539.9[b]
5	B_2	2843.4	2968.0	2159.7	2233.0
6	B_2	1251.2	904.0	990.4	705.0

B. Lowest Singlet Electronic States of Formaldehyde

state label	symmetry (C_{2v})	transition	vertical excitation energy, eV
a	A_1		0
b	A_2	$n_p \rightarrow \pi_2$	4.3
3	B_2	$n_p \rightarrow \sigma_2$	7.1
4	A_1	$\pi_1 \rightarrow \pi_2$	8.0
5	B_1	$\sigma_1 \rightarrow \pi_2$	~10.0

[a] (A) Frequencies of the six normal modes in the S_0 ($^1A_1$) and S_1 ($^1A_2$) electronic states of H_2CO and D_2CO. (B) Symmetry, orbital change, and vertical excitation energy associated with each of the four lowest electronic absorption features in H_2CO. [b] Double-minimum potential eigenfunctions have been expressed as a sum of harmonic oscillator wavefunctions of the given frequency.

As interesting as is the dramatic variation of τ_{S_1} with rotational level, the qualitatively more significant fact confirmed by the Weisshaar/Moore experiments is that, *in the absence of collisions, S_1-formaldehyde decays* (on the average) *more than 20 times faster than it would if it simply radiated.* (Here we have taken (τ_{S_1}) average $\sim$150 ns[30] and $\tau_{S_1}^{rad}$ $\sim$3000 ns.[46]) In the case of D_2CO, on the other hand, τ_{S_1} does *not* vary with rotational level and is approximately equal to τ_S^{rad}. Thus the first task of any theory of the formaldehyde photodissociation will be to explain the fast, collisionless, nonradiative decay of zero-point S_1-H_2CO (and its absence in D_2CO).

C. "Time Lag" to Products

The one other experimental datum that we choose to feature comes from the work of Houston and Moore.[29] After exciting H_2CO to about 1800 cm^{-1} above its S_1 origin they time-resolved the appearance of CO product. This was done by either monitoring the fluorescence from $v = 1$ or following the absorption by $v = 0$ of a probe CO laser's light. The CO product was observed to grow in exponentially with a rate, k_{CO}, proportional to pressure, P. A linear extrapolation to $P = 0$ gave $k_{CO} = 0$. At the lowest pressure studied, $P = 0.1$ torr, k_{CO} was as small as 0.25×10^6 s^{-1}, implying $\tau_{CO} > 4000$ ns. That is, it appears that we have to wait more than a microsecond to see CO growing in, even though the large (overwhelming) majority of S_1 states decay on time scales as short as 150 ns. The slope of the k_{CO} vs. P curve is $\sim 1.7 \times 10^6$ s^{-1} torr^{-1}, corresponding to a collisional rate of about one-sixth gas kinetic. The same behavior is observed when S_1 is excited[47] within a couple hundred cm^{-1} of its origin, and is independent of whether inert collision partners are added.

More explicitly, for each pressure studied, it was found that the amplitude of CO product was negligible at short times, i.e., for $t \lesssim 100$ ns. Most of the CO was seen to grow in on a much longer time scale, $1/k_{CO}$. At long times the CO signal levels off to a constant, $A(\infty)$, which is large compared to the short time ("background") $A(0)$. The short-time $A(0)$ is so small, in fact, that it is lost in the noise of the detector. The long-time amplitude, $A(\infty)$, is roughly proportional to pressure, as is the rate k_{CO}. Thus as the gas pressure of H_2CO is lowered from

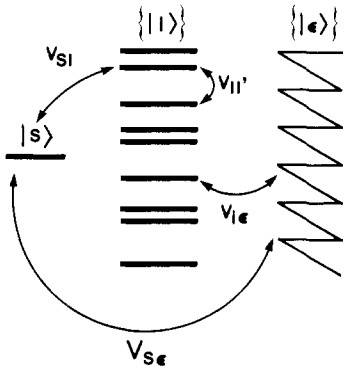

Figure 2. Schematic diagram of coupling between the optically excited initial state (s), the vibrationally "hot" bound states ($\{|I\rangle\}$) of the ground electronic configuration, and the dissociation continuum (ϵ).

10 to 0.1 torr, both $A(\infty)$ and k_{CO} decrease accordingly. At $P = 0.1$ torr, A(CO) disappears into the noise, but $A(0)/A(\infty)$ could be as large as 0.1 at this point. Carrying out this same experiment with enhanced sensitivity, i.e., extending the pressures down to tenths of a millitorr, might well show that $A(\infty)/P$ is no longer constant but instead begins to increase as P is lowered. Simultaneously we might find that $A(0)/A(\infty)$ tends to unity—that is, the long-time, pressure-dependent component disappears—the time lag does not survive.

In any case, the inescapable conclusion that must be drawn from the present observations is that *at pressures on the order of 0.1 torr, there is at least a microsecond time lag between the fast (0.15 μs) decay of S_1 and the appearance of H_2 + CO products*. As we shall see, there appears to be a fundamental inconsistency between the existence of this time lag at $P \sim 0.1$ torr and the presence of the collisionless ($P \lesssim 0.0001$ torr) nonradiative relaxation of S_1.

III. Theory

A. Elert, Heller, and Gelbart

In what follows we shall ignore the presence of the lowest triplet and consider only the coupling between S_1 and S_0. Figure 2 depicts schematically the three manifolds of states associated with these two electronic configurations. $|S\rangle$ refers to the optically excited ro-vibrational level in S_1. The $\{|I\rangle\}$ are the vibrationally "hot" levels of S_0 which are isoenergetic with $|S\rangle$ but which do not have sufficient energy in the reaction coordinate for dissociation to occur. The $\{|\epsilon\rangle\}$ are the continuum states which describe the molecule flying apart in S_0 with relative kinetic energy ϵ.

$|S\rangle$, $\{|I\rangle\}$ and $\{|\epsilon\rangle\}$ are eigenfunctions of an approximate molecular Hamiltonian which excludes the nuclear kinetic energy $T(Q)$ and the vibrational anharmonicity $V_{S_0}^{anh}(Q)$ associated with the S_0 potential energy surface. It is $T(Q)$ which mixes $|S\rangle$ and $\{|I\rangle\}$ [hence $v_{SI} = \langle S|T(Q)|I\rangle$] and $|S\rangle$ and $|\epsilon\rangle$ [$v_{S\epsilon} = \langle S|T(Q)|\epsilon\rangle$]. These are the nonadiabatic interactions due to the breakdown of the separation of electronic and nuclear motions. The $\{|I\rangle\}$ and $\{|\epsilon\rangle\}$, on the other hand, all belong to the same (S_0) configuration and thus are mixed by $V_{S_0}^{anh}(Q)$ [hence $v_{II'} = \langle I|V_{S_0}^{anh}|I'\rangle$ and $v_{I\epsilon} \equiv \langle I|V_{S_0}^{anh}|\epsilon\rangle$]. As soon as we pick a particular basis of functions to represent the above states, all their energies and coupling matrix elements follow. Before doing this we discuss briefly the means by which we shall calculate the time evolution of the initially prepared (optically excited) state.

Because of the presence of the continua we are confronted with an (uncountably) infinite dimensional problem. However, *if* we are content to look only at the probabilities of being in any one of the *bound* states, and *if* $v_{S\epsilon}$ and $v_{I\epsilon}$ are sufficiently slowly varying functions of ϵ, then—to a very good approximation[40,48]—the dynamical problem reduces to a finite dimensional one. The continuum, instead of appearing explicitly, simply adds pure imaginary contributions to the matrix representation of the molecular Hamiltonian (H) in the basis of bound states ($|S\rangle$ and $\{|I\rangle\}$).

More explicitly, it can be shown[40,48] that the time-dependent amplitudes determining the excited-state wave function

$$|\Psi(t)\rangle = a_0(t)|S\rangle + \sum_{I=1}^{N} a_I(t)|I\rangle \tag{1}$$

are governed by the simple equation of motion

$$i\hbar \frac{d}{dt}\begin{bmatrix} a_0(t) \\ a_1(t) \\ \vdots \\ a_N(t) \end{bmatrix} = H_{eff}\begin{bmatrix} a_0(t) \\ a_1(t) \\ \vdots \\ a_N(t) \end{bmatrix} \tag{2}$$

Here H_{eff}, the *effective* Hamiltonian matrix, is defined by its representation in the bound state basis, $\{|m\rangle\} \equiv |S\rangle$, $\{|I\rangle\}$:

$$(H_{eff})_{mm'} \equiv H_{mm'} - \frac{i}{2}\Gamma_{mm'} \tag{3}$$

$H_{mm'}$ is simply $\langle m|H|m'\rangle$, the matrix element of either $T(Q)$ or $V_{S_0}^{anh}(Q)$, according to whether or not m and m' belong to different electronic configurations: e.g., $H_{SI} = v_{SI} = \langle S|T(Q)|I\rangle$ and $H_{II'} = v_{II'} = \langle I|V_{S_0}^{anh}(Q)|I'\rangle$. $\Gamma_{mm'}$, on the other hand, is the *damping* matrix, defined[40,48] by

$$\Gamma_{mm'} = 2\pi\langle m|H|\epsilon\rangle\langle\epsilon|H|m'\rangle \tag{4}$$

For $m = S$, $\langle m|H|\epsilon\rangle \rightarrow v_{S\epsilon} = \langle S|T(Q)|\epsilon\rangle$, etc.

Note that the diagonal matrix elements of Γ are simply the widths of the bound states due to dissociation, whereas the *off*-diagonal $\Gamma_{mm'}$'s describe the quantum mechanical interference effects due to coupling of the bound states *through* the continuum. [Direct continuum–continuum interactions are ignored: these give rise to changes in the internal excitation of the fragments as they separate.] Note that in writing (4) we have suppressed the fact that there are in general a large number of continua which have to be considered, one for each possible distribution (see below) of vibrational energy in the diatomic products. Thus the continuum $\{|\epsilon\rangle\}$ should carry a subscript which identifies it as one of many channels, and eq 4 should be replaced by the sum $2\pi\sum_k\langle m|H|\epsilon_k\rangle\langle\epsilon_k|H|m'\rangle$.

Computation of the $H_{mm'}$ and $\Gamma_{mm'}$ matrix elements, as described below, and subsequent diagonalization of H_{eff} lead to a direct solution for $|a_0(t)|^2$, $\sum_{I=1}^{N}|a_I(t)|^2$ and $1 - \sum_{I=0}^{N}|a_I(t)|^2$, the time-dependent probabilities of being in any one of the three manifolds of interest.

Implicit already in our description of coupling energies is a choice of basis states formed from Born–Oppenheimer (adiabatic) products of electronic and vibrational wave functions. We write the vibrational factors in turn as products of harmonic oscillator states, one for each of the six normal modes of motion. Multiplied by $\Psi_{S_1}(qQ)$ and $\Psi_{S_0}(qQ)$ these describe the bound states $|S\rangle$ and $\{|I\rangle\}$, respectively. The nuclear-coordinate dependences of the electronic wave functions $\Psi_{S_1}(qQ)$ and $\Psi_{S_0}(qQ)$ are computed by using Herzberg–Teller theory through second order—the necessary *crude* Born–Oppenheimer (i.e., equilibrium configuration) electronic wave functions are available from ab initio calculation (e.g., see ref 5) and the nuclear coordinate transformations are known from the normal mode analyses (e.g., see ref 49). Details and discussion of this calculation of $\Psi_{S_1}(qQ)$ and $\Psi_{S_0}(qQ)$ are given in Appendix A, where our results are compared against other, independent estimates of the nuclear-coordinate dependence of the electronic wave functions.

Table III

basis state	shifted energy, cm^{-1}	initial state matrix element, cm^{-1}	basis state	shifted energy, cm^{-1}	initial state matrix element, cm^{-1}
3 1 1 2 1 8	28313.1	-2.486623E-04	1 0 8 4 0 7	28324.4	1.633688E-02
0 4 8 0 2 1	29712.1	1.935354E-02	3 0 0 8 1 8	28325.1	-2.665856E-04
2 5 0 0 3 2	28313.3	-4.644060E-03	0 2 5 2 5 0	28300.0	1.788407E-03
1 7 0 10 1 2	28311.9	-5.301349E-01	2 0 5 8 1 4	28325.3	1.360768E-02
0 3 0 2 4 9	28311.7	-8.145123E-06	0 4 10 4 0 1	28325.3	2.024450E+00
2 1 5 4 0 7	28311.4	-2.296806E-02	0 10 3 0 1 0	28325.4	1.298714E+00
0 1 4 0 4 7	28311.2	-1.335653E-05	5 0 3 2 0 3	28325.5	-2.963149E-03
1 5 0 0 5 0	28314.4	-5.832518E-03	2 0 0 4 2 11	28299.1	1.246736E-04
0 5 0 0 6 1	28314.4	8.554115E-05	0 2 10 2 0 5	28298.9	4.919396E-02
1 2 8 6 0 3	28314.5	3.102839E-01	2 5 0 6 0 7	28325.9	-1.008829E-01
0 8 3 2 0 5	28310.6	4.983345E-01	2 4 3 4 0 5	28327.0	-1.945418E-01
3 2 2 2 1 8	28310.6	-4.427616E-04	3 2 3 12 0 1	28327.1	1.282550E-21
1 5 5 2 1 2	28314.7	-2.236482E-01	0 1 2 0 7 2	28298.1	-3.356695E-05
0 0 3 4 0 17	28310.4	-2.214314E-05	0 1 3 6 3 8	28298.0	-1.536225E-04
1 5 1 4 3 2	28310.4	4.893154E-02	4 1 2 4 1 2	28328.2	-6.240048E-03
2 2 5 2 1 4	28315.1	2.041624E-02	0 1 1 6 5 6	28296.9	8.549139E-05
2 1 2 10 3 0	28315.1	-6.423921E-02	0 0 3 0 2 15	28296.5	4.758093E-07
2 3 3 8 1 2	28309.8	2.077980E-01	1 5 3 0 1 6	28296.4	-5.764410E-03
3 0 2 5 1 6	28315.5	-1.033741E-03	0 4 9 0 1 2	28328.8	6.656319E-02
3 2 1 6 0 7	28315.6	1.032736E-02	1 5 4 2 2 1	28328.9	-8.557840E-02
1 0 0 8 4 7	28309.3	2.204415E-04	0 9 3 0 1 2	28329.2	2.228511E-01
3 3 5 0 0 3	28316.1	6.583714E-03	1 0 14 0 1 0	28329.7	-1.484848E-02
1 1 11 6 0 1	28309.1	3.432924E-01	0 9 0 6 2 1	28295.4	-5.227185E-01
0 0 0 4 5 10	28308.8	8.709859E-06	2 4 2 0 1 6	28295.3	1.911235E-03
1 8 0 10 1 0	28308.7	-2.866375E-00	4 0 4 2 0 5	28329.9	1.059110E-03
1 1 3 6 2 7	28308.4	-2.985835E-03	0 0 10 4 0 7	28295.1	3.295651E-03
1 0 8 8 0 5	28317.0	5.031768E-02	0 5 7 8 0 1	28330.2	4.400851E+00
2 0 8 6 2 1	28308.0	2.588983E-02	1 0 4 6 2 7	28294.9	-1.920264E-03
0 2 3 4 4 5	28317.3	2.897398E-04	3 0 7 8 0 1	28330.3	5.872954E-02
3 0 4 4 0 7	28307.4	3.066010E-03	4 3 6 10 0 1	28294.7	6.488168E-02
1 0 2 2 4 7	28307.4	1.030963E-04	1 9 6 0 3 14	28330.5	4.834331E-07
1 0 6 2 11 10	28307.2	-3.362141E-04	1 1 2 4 1 12	28294.6	-3.174801E-04
1 1 2 10 4 1	28307.0	6.101377E-03	1 2 6 6 2 1	28330.8	-7.673418E-02
4 0 0 12 0 5	28318.8	1.735958E-03	2 0 10 6 0 1	28294.4	-1.925800E-01
0 3 3 0 3 8	28318.8	-1.145932E-04	1 2 2 0 5 2	28294.1	-5.365690E-04
0 2 3 4 1 12	28306.2	8.097279E-05	0 2 5 8 3 2	28331.4	6.888670E-04
2 2 10 0 0 1	28319.2	-4.462192E-02	2 3 2 4 3 0	28331.9	-1.540954E-01
0 5 3 2 4 1	28305.2	7.828242E-03	4 2 0 6 0 5	28332.3	8.310832E-03
1 0 3 10 4 1	28305.7	3.376178E-03	2 2 6 10 0 1	28292.6	-5.991775E-01
0 0 6 8 4 1	28319.6	-1.267526E-04	1 3 2 4 4 1	28292.5	1.229312E-02
1 1 6 4 1 6	28319.7	-1.019118E-02	0 6 5 8 1 0	28331.7	-2.346834E+00
1 7 1 4 2 1	28319.8	-1.575103E-01	0 1 6 8 4 1	28292.2	1.693613E-03
1 2 1 10 4 1	28304.5	6.947819E-03	1 7 1 2 0 7	28292.2	5.974888E-02
1 3 2 0 3 6	28320.8	3.970036E-04	0 2 2 4 5 4	28333.5	3.023361E-04
0 1 5 2 2 9	28304.4	-7.417060E-05	1 4 0 6 2 7	28291.7	-7.934099E-03
2 5 5 0 1 0	28304.0	1.429002E-01	0 1 7 4 2 5	28333.9	-2.774864E-03
2 4 0 10 1 4	28321.2	6.057780E-02	0 4 6 10 0 3	28291.2	8.858707E-01
0 5 6 2 2 1	28303.0	-1.207119E-01	0 4 9 4 1 0	28291.1	-7.677952E-01
0 5 3 0 2 7	28321.9	8.571664E-04	1 2 2 6 2 7	28291.0	-4.565493E-03
2 1 0 8 1 10	28303.2	6.785283E-04	3 1 9 0 0 1	28290.9	5.284256E-03
2 0 8 4 1 2	28302.5	3.678451E-02	0 3 5 10 1 4	28290.7	-1.750706E-02
3 1 5 10 0 1	28302.4	1.060252E-01	0 1 10 2 3 0	28335.0	-4.121105E-03
0 1 6 8 3 2	28322.8	-3.012883E-03	2 0 0 8 4 3	28290.2	-1.407395E-03
2 3 2 10 0 5	28302.3	-1.359547E-01	3 2 0 2 3 2	28289.9	3.760386E-03
2 1 4 0 1 8	28302.2	1.781770E-04	1 6 2 10 0 3	28289.5	6.819983E-01
0 1 2 0 6 5	28323.0	2.258401E-06	1 6 3 8 1 0	28289.3	-2.007615E+00
1 1 2 6 3 6	28302.2	1.933272E-03	0 7 4 0 1 4	28335.9	4.282427E-02
2 0 10 2 0 3	28323.2	-3.811046E-02	1 2 0 2 6 1	28288.7	-8.691888E-04
1 2 7 10 1 0	28323.5	-5.759666E-01	0 4 6 6 0 5	28335.8	4.156574E-01
0 2 10 4 1 2	28323.6	-3.447529E-02	2 3 1 10 1 4	28337.1	3.910793E-02
0 0 10 10 1 2	28323.8	7.871386E-03	1 4 3 8 2 1	28288.0	-1.221757E-01
0 1 4 8 5 0	28323.9	3.694912E-03	1 3 1 0 5 2	28337.3	-6.455321E-04
0 5 8 2 0 1	28324.1	2.528989E+00	0 7 0 0 4 3	28287.8	-6.189040E-04
3 2 2 0 1 6	28301.0	-1.635104E-04	2 4 1 6 0 7	28338.1	-6.823627E-02

[a] Each S_0 basis state listed on the left is specified by the number of quanta in the six normal modes of vibration; e.g., w = 3, 1, 1, 2, 1, 8 refers to three quanta in ν_1 (the symmetric CH stretch), one in ν_2 (the CO stretch), and so on. The "shifted energy" entries are the expectation values of $V_{S_0}^{anh}(Q)$ with respect to these zero-order product states. Finally the right-most column gives the matrix elements $\langle \Psi_{S_1 v=0} | T(Q) | \Psi_{S_0 w} \rangle$.

In order to differentiate between the bound ($\{|I\rangle\}$) and continuum ($\{|\epsilon_k\rangle\}$) states belonging to S_0 we need to define the reaction coordinate. We take ν_3 as our reaction coordinate: the symmetric, in-plane, bend (the "scissoring motion"). The reaction coordinate should include some CH stretch as well—the hydrogen atoms must not only come closer to each other, but must also separate from CO, before H_2 is formed—but our simpler choice suffices for the present discussion.

The ν_3 motion in S_0 is described by a *Morse* oscillator (mo) $[V_{\nu_3}(x) = D\{1 - \exp(-\alpha x)\}^2]$, where D is the barrier height against dissociation and α is chosen to give the observed ν_3 fundamental frequency. The $\nu_{l\neq 3}$ motions are described by *harmonic* oscillators (ho). Thus the $\{|I\rangle\}$ are constructed by enumerating all states corresponding to $\mathbf{w} = w_1, \ldots, w_6$ such that $\hbar\omega_3(w_3 + 1/2) < D$. These $\{w_i\}_{i=1 \ldots 6}$ describe S_0 states with the energy in the reaction coordinate insufficient for dissociation: their wave functions and energies are given by

$$|I\rangle = \Psi_{S_0}(qQ)\prod_{i=1}^{6}\chi^{ho}_{S_0 w_i}(Q_i) \leftrightarrow E_I = \sum_{i=1}^{6}\hbar\omega_i(w_i + 1/2) \quad (5)$$

Each continuum, on the other hand, is associated with $\{w_i\}_{i\neq 3}$ such that $[\sum_{l\neq 3}^{6}\hbar w_l(w_l + 1/2)] < [E_{S_1}^{ex} - D]$, i.e., with each vibrational distribution which leaves *at least* energy D in ν_3. ($E_{S_1}^{ex}$, the energy of the exciting light, defines the total molecular energy available.) Thus the kth continuum is specified by

$$|\epsilon_k\rangle = \Psi_{S_0}(qQ)\chi^{mo}_{S_0\epsilon_k}(Q_3)\prod_{l\neq 3}^{6}\chi^{ho}_{S_0 w_l}(Q_l) \quad (6)$$

The translational energy available to ν_3 is just

$$\epsilon_k = [E_{S_1}^{ex} - D] - [\sum_{l\neq 3}^{6}\hbar\omega_l(w_l + 1/2)] \quad (7)$$

Note that $\chi^{mo}_{S_0\epsilon_k}$ is the well-known, unbound, solution (asymptotic kinetic energy ϵ_k) of the Morse oscillator. Finally, our remaining basis state (S) is defined by

$$|S\rangle = \Psi_{S_1}(qQ)\prod_{l=1}^{6}\chi^{ho}_{S_1 v_l}(Q_l) \quad (8)$$

where the $\{Q_l\}$ now refer to the normal modes *on the S_1 surface*.

With $|S\rangle$, $\{|I\rangle\}$, and $\{|\epsilon_k\rangle\}$ defined explicitly as above, the matrix elements of the nuclear kinetic energy, $T(Q) = -\hbar^2\sum_{l=1}^{6}\partial^2/\partial Q_l^2$ can be straightforwardly evaluated. These calculations are outlined in Appendix B. Of particular interest are the $\langle S|T(Q)|I\rangle \equiv v_{SI}$ interaction energies. Recall that the $\{v_{SI}\}$ are the fundamental quantities in the primordial Bixon–

Table IV

	states		interaction energy, cm^{-1}
1	7	117	-7.539920D-15
2	7	322	1.048152D+02
3	7	352	-2.148260D-04
4	8	176	-4.248756D-03
5	23	144	8.757702D+01
6	23	310	-4.115543D-03
7	23	363	-7.124608D-01
8	23	429	3.675233D-01
9	35	176	-1.236165D-01
10	39	176	1.666441D-05
11	41	66	2.237093D-03
12	41	366	-5.473184D+00
13	41	397	-6.215807D-06
14	41	435	1.361131D-02
15	42	419	4.834173D-14
16	42	486	-7.705213D-18
17	46	134	-4.260387D-01
18	46	180	2.410565D+01
19	46	323	4.165602D+01
20	48	359	-3.590095D-12
21	50	463	3.303512D-13
22	56	113	4.969536D+01
23	56	201	-6.129314D-02
24	56	413	-1.139184D-14
25	65	367	-1.454371D-04
26	70	96	-1.578858D-05
27	75	90	-1.720200D-04
28	75	211	1.277166D-06
29	75	294	-5.937987D-06
30	75	311	-2.343589D-08
31	78	180	-1.885054D-14
32	96	136	3.778975D-03
33	96	245	-5.200898D-05
34	96	254	1.144960D+01
35	96	358	-9.854844D-01
36	96	451	-8.871555D-06
37	98	367	-1.194563D+00
38	99	290	-1.351412D-02
39	113	201	2.120404D-01
40	134	180	-3.948437D+01
41	149	151	-3.490853D-12
42	162	217	6.208949D-05
43	162	403	-1.715612D-01
44	175	217	8.356959D-14
45	176	188	-3.637656D-04
46	176	321	2.379172D-02
47	177	432	-6.955717D-05
48	180	323	-8.441596D+02
49	201	409	1.851494D-01
50	206	360	-1.111924D-01
51	206	441	2.931766D-01
52	206	482	4.263284D+01
53	217	403	1.703259D+01
54	255	290	1.905814D-03
55	255	369	-2.837242D-06
56	255	434	4.700665D+01
57	290	434	-1.357616D-04
58	314	356	8.356959D-14
59	318	367	3.923370D-03
60	356	358	-1.678384D-03
61	357	367	2.251544D-04
62	367	370	-5.522623D-08
63	367	396	-2.249991D-15
64	406	463	-8.289797D+02
65	424	476	1.448142D-03
66	476	495	2.855910D-02

[a] Matrix elements of $V_{S_0}^{anh}(Q)$ between different zero-order S_0 vibronic states ($\{\Psi_{S_0 W}\}|l\rangle\}$). The 66 interaction energies shown here are those corresponding to the pairs of l states retained in the convergence criteria described in Appendix C. (Their numberings, e.g., "7-117", "7-322", refer to the labeling scheme devised in ref 40.)

Jortner model of radiationless transitions. Table III shows our calculated values of the $\{v_{Sl}\}$ for the S_0–S_1 interaction in formaldehyde. The matrix elements are seen to fluctuate dramatically in both magnitude and sign, in marked contrast to the slow variation usually assumed in the analyses of electronic intramolecular relaxation processes. As shown elsewhere,[50] however, the fluctuations in $\{v_{Sl}\}$ do not destroy the qualitative behavior originally predicted by the constant coupling model.

Similarly, having defined the basis states $|S\rangle$, $\{|l\rangle\}$, and $\{|\epsilon_k\rangle\}$, we can compute all of the matrix elements involving $V_{S_0}^{anh}(Q)$. For $V_{S_0}^{anh}(Q)$ we use an analytic fit to the ab initio S_0 surface of Morokuma et al. These calculations are also described in Appendix B; typical results for the anharmonic coupling energies $\langle l|V_{S_0}^{anh}(Q)|l'\rangle \equiv v_{ll'}$ are shown in Table IV. From these v_{Sl}, $v_{S\epsilon_k}$, $v_{ll'}$, and $v_{l\epsilon_k}$, we construct the $H_{mm'} - (i/2)\Gamma_{mm'}$ matrix (see eq 3 and 4) whose diagonalization leads directly to $P_{S_1}(t) \equiv |a_0(t)|^2$ and $P_{diss}(t) \equiv 1 - |a_0(t)|^2 - \sum_{l=1}^{N} |a_l(t)|^2$.

It is important to note that there is nothing special about the Born–Oppenheimer or normal mode approximations which we have used to construct our basis; this choice is admittedly arbitrary. There is no reason to expect the vibrationally hot S_0 levels to be well described by products of harmonic oscillator products. Surely it would be better to use Morse potential descriptions of *local* (rather than normal) modes and to account for *changes* in the natural coordinates as we go from H_2CO–S_1 to $(H_2 + CO)$–S_0. Nor does our Herzberg–Teller treatment provide the most accurate way to collect the nuclear-coordinate dependence of the electronic wave functions. van Dijk et al., for example, have calculated $\Psi(q)$ directly for all Q's of interest—as mentioned earlier, *their* approximation is to assume that the potential-energy surfaces and electronic matrix elements (arising from $T(Q)$) are separable with respect to the normal coordinates. But we do not need to worry about having chosen the "best" basis, since we can show that our dynamics calculations are independent of the particular choice of basis. We "simply" increase the size of the $\{|l\rangle\}$ set until we find $P_{S_1}(t)$ and $P_{diss}(t)$ to be invariant, i.e., until the calculations have converged; this procedure is described in Appendix C.

We have performed a large number of calculations of $P_{S_1}(t)$ and $P_{diss}(t)$ for different vibrationally excited levels of S_1-H_2CO and S_1-D_2CO: the details are given in ref 40. For our present purposes we need only cite the following:

(i) $[E_{S_1}^{ex} - D] > 0$. When the molecular excitation energy exceeds the barrier against formation of products (by, say, a few thousand cm^{-1}), $|S\rangle$ is found to decay on a 100-ns time scale in the case of H_2CO, and approximately 20 times slower for D_2CO; these results are in good accord with experiment. However, $P_{diss}(t)$ is found to grow in on about the same time scale. That is, there is no dramatic time lag.

(ii) $E_{S_1}^{ex} < D$. In this case we do not find any nonradiative decay of S_1 on observable time scales. This result is in agreement with calculations by van Dijk et al. (see below) in which the $S_1 \sim\!\!\rightarrow S_0$ internal conversion was treated in the absence of dissociation ($E_{S_1}^{ex} < D$).

Thus we have the basic dynamical paradox. If dissociation is indirectly responsible (see below for discussion) for the nonradiative decay of S_1, then how can a time lag be explained? If dissociation is *not* involved, then how can S_1 undergo such a fast radiationless relaxation? These features of the photodissociation dynamics should arise in the case of many other "intermediate" sized molecules as well.

B. van Dijk, Kemper, and Buck

van Dijk, Kemper, and Buck and their co-workers have provided a most comprehensive theoretical study of the radiative and nonradiative processes associated with the S_0–S_1 $^1(n \rightarrow \pi^*)$ transition in formaldehyde. Their program involves a completely ab initio determination of all the relevant molecular properties. In particular they take advantage of the fact that the integrals involved in the electronic (nonadiabatic) coupling matrix elements, which determine the *non*radiative relaxation of S_1, are completely equivalent to the dipole acceleration electronic transition moments arising in the radiative decay. Furthermore they calculate directly the nuclear-coordinate dependences of the electronic wave functions rather than piecing them together from a low-order Herzberg–Teller expansion.

More explicitly, consider the following contribution to the nonadiabatic [nuclear kinetic energy, $-\hbar^2 \sum_{l=1}^{6} \partial^2/\partial^2 Q_l^2 \equiv T(Q)$] coupling between the S_0 and S_1 electronic configurations:

$$C_{10}(Q) = \sum_{l=1}^{6} \left\langle \Psi_{S_1}(qQ)\left|-i\hbar\frac{\partial}{\partial Q_l}\right|\Psi_{S_0}(qQ)\right\rangle_q \left(-i\hbar\frac{\partial}{\partial Q_l}\right) = -\hbar^2 \sum_{l=1}^{6} \frac{\left\langle \Psi_{S_0}(qQ)\left|\frac{\partial U}{\partial Q_l}(qQ)\right|\Psi_{S_1}(qQ)\right\rangle_q \frac{\partial}{\partial Q_l}}{E_{S_0}(Q) - E_{S_1}(Q)} \equiv -\hbar^2 \sum_{l=1}^{6} \frac{V_l^{10}(Q)}{E_0(Q) - E_1(Q)} \frac{\partial}{\partial Q_l} \quad (9)$$

Here U is the full potential energy of the interacting electrons and nuclei and $E_0(Q)$ and $E_1(Q)$ are the adiabatic electronic

eigenvalues of the S_0 and S_1 states. The *total* interaction energy between the wth and vth vibrational levels of the S_1 and S_0 states, respectively, is accordingly

$$-\hbar^2 \left\langle \chi_{S_1 v}(Q) \left| \frac{\sum_{i=1}^{6} V_i^{10}(Q) \frac{\partial}{\partial Q_i}}{E_0(Q) - E_1(Q)} \right| \chi_{S_0 w}(Q) \right\rangle_Q \equiv v_{S_1 v, S_0 w} \quad (10)$$

The vibrational wave functions $\chi_{S_1 v}$ are as usual the eigensolutions to the Schrödinger equation for effective nuclear motion in the S_1 state:

$$[T(Q) + E_1(Q)]\chi_{S_1 v}(Q) = E_{S_1 v}\chi_{S_1 v}(Q) \quad (11)$$

(And similarly for $\chi_{S_0 w}$.) Thus we need "only" determine $\Psi_S(qQ)$, $\Psi_{S_1}(qQ)$, $E_0(Q)$, and $E_1(Q)$.

In order to proceed with their ab initio determination, van Dijk et al. introduce a key simplification. They assert that both $E_n(Q)$ and $V_i^{10}(Q)/[E_0(Q) - E_1(Q)]$ are separable with respect to the six normal coordinates, $\{Q_i\}_{i=1,2,\ldots,6}$. Accordingly they write

$$E_n(Q) = E_n(Q = 0) + \sum_{i=1}^{6} E_n^i(Q_i) \quad (12)$$

and

$$\frac{V_i^{10}(Q)}{E_0(Q) - E_1(Q)} = V_i^{10}(Q = 0) + \sum_{i=1}^{6} V_{i,i'}^{10}(Q_{i'}) \quad (13)$$

From (12) it follows that eq 11 is separable into six one-dimensional vibrational motion problems; $\chi_{S_1 v}(Q)$, for example, can be written as a product

$$\prod_{i=1}^{6} \chi_{S_1 v}^i(Q_i)$$

Here each $\chi_{S_1 v}(Q_i)$ is determined numerically as the appropriate eigenfunction of the one-dimensional potential $E_1^i(Q_i)$. Note that assumption 12 is not to be confused with the *harmonic* approximation; (12) requires "only" that the potential energy be *separable* with respect to the Q_i's—"diagonal" anharmonic terms to all orders are still included. Similarly, assumption 13 is considerably weaker than the usual "Condon approximation" which has often been invoked[51] to treat internal conversion processes.

The $V_i^{10}(Q)$ defined in eq 9 can be expressed (see Appendix A) entirely in terms of $\Psi_{S_1}(qQ) - \Psi_{S_0}(qQ)$ matrix elements of the electric field operators

$$\sum_e \frac{\mathbf{q}^e - \mathbf{S}^n}{r_{en}^3} \equiv \mathcal{E}_n$$

Here $\mathbf{q}^e$ and $\mathbf{S}^n$ denote the vector positions of the eth electron and nth nucleus, and r_{en} is the distance between them. More explicitly, we can write (see Appendix A)

$$V_i^{10}(Q) = \sum_n \sum_j \frac{\partial S_j^n}{\partial Q_i} Z_n \left\langle \Psi_{S_1}(qQ) \left| \sum_e \frac{q_j^e - S_j^n}{r_{en}^3} \right| \Psi_{S_0}(qQ) \right\rangle_q \quad (14)$$

where the subject j labels the (x, y, or z) Cartesian component $\mathbf{q}^e$ and $\mathbf{S}^n$, Z_n is the nth nuclear charge, and $\partial S_j^n/\partial Q_i$ are the elements of the Jacobian transformation from normal to Cartesian coordinates. van Dijk et al. have computed the 12 Cartesian components (three per atom) of the electric field operator at each point (nuclear configuration) for which the S_0 and S_1 wave functions was calculated. With assumptions 12 and 13 in mind, about 14 points per normal coordinate were considered. The atomic orbitals are chosen to be a contracted Gaussian basis set of double zeta quality; a single molecular orbital set is used to describe both the S_0 and S_1 states. As many as 175 configurations were included in the CI.

Recall from section IIIA, that the time-dependent amplitudes governing the excited-state wave function (eq 1) follow [see (2)] from a diagonalization of the effective Hamiltonian matrix (eq 3). The calculation of van Dijk et al. involves only *bound* states of S_0; accordingly, the damping matrix defined by (4) is identically zero. Furthermore, $v_{ll'} \equiv 0$ since—see assumption 12—"off-diagonal" ("coupling") anharmonicity has been neglected. Thus

$$H_{\text{eff}} \longrightarrow \begin{pmatrix} E_{S_1} & \cdots & V_{Sl} & \cdots \\ \vdots & \ddots & & \\ V_{Sl} & & E_l & \\ \vdots & & & \ddots \end{pmatrix} \quad (15)$$

The v_{Sl}'s are given by the $v_{S_1 v, S_0 w}$'s in (10), as simplified in the above discussion; the E_l's are obtained similarly from the Q_i cross sections of the S_0 surface. Matrix 15 has eigenvalues E_m' and eigenvectors $\{f_m\}$ whose overlaps with $|S\rangle$ are $\{a_m\}$. It follows that the time-dependent probability of being in the initial state $|S\rangle$ is

$$P_S(t) = |\sum_m |a_m|^2 \exp(-iE_m' t/\hbar)|^2 \quad (16)$$

van Dijk et al. find results for the v_{Sl}'s which are qualitatively similar to those discussed earlier in Table III. Also, their density of $|l\rangle$ levels—including the effects of "dlagonal anharmonicity"—is essentially the same as that found for the purely harmonic basis treated in section IIIA. Most significantly, their calculations confirm the conclusion that S_1-H_2CO behaves like a "small" or "resonance-case" molecule;[52] in the absence of continuua, no nonradiative decay is observable on a 100-ns time scale. [Instead, $P_s(t)$ simply undergoes picosecond oscillations.]

IV. Discussion: Mechanism Dilemmas

A. Tunneling

In the above discussion it has been assumed implicitly that no dissociation can occur if $E_{S_1}^{ex} < D$. Indeed if the reaction coordinate is described by a Morse potential, then no dissociation is possible in this case. But (see Figure 1) a more reasonable one-dimensional potential would be one which rises to a maximum at intermediate displacements and then falls back down to zero as the products separate. (Recall that ground state H_2 + CO has essentially the same energy as S_0-H_2CO.) In this latter case, quantum mechanical tunneling can lead to dissociation even when $E_{S_1}^{ex} < D$.

Miller[53] has recently included tunneling corrections to the usual statistical theory of unimolecular reactions. Assuming that the reaction coordinate is separable, he uses the one-dimensional barrier potential computed by Goddard and Schaefer[4] for the minimum energy $H_2CO \rightarrow H_2 + CO$ pathway. For molecular energies lying about 2000 cm^{-1} below the barrier, he finds tunneling rates as high as 6×10^6 s^{-1}; at 1000 cm^{-1} below the barrier, they are already an order of magnitude larger. These are of course only crude estimates of the formaldehyde tunneling rates since the full many-dimensionality of the problem has not been considered. Nevertheless we can incorporate this result into our earlier calculational scheme as follows.

Recall that the damping matrix elements $\Gamma_{mm'}$ arise from coupling of the bound states to the continuum channels. But, for $E_{S_1}^{ex} < D$ and a Morse description of the reaction coordinate, all the $\Gamma_{mm'}$'s were zero since the continua were simply not

accessible. In the case of a *barrier* potential, on the other hand, the continua are accessible via tunneling; thus we can set each $\Gamma_{\parallel}/\hbar$ equal to a rate on the order of 10^6–10^7 s^{-1}. Using our original estimates of the $H_{mm'}$ matrix elements, and diagonalizing the resulting $\boldsymbol{H}_{eff}$ matrix, we find that $P_{S_1}(t)$ decays on a 100-ns time scale. Thus, even with $E_{S_1}^{ex}$ lying below D—which is almost certainly the experimental situation—we can account for the fast nonradiative relaxation of S_1. Similarly, the dramatic decrease (factor of ~20) in $1/\tau_{S_1}$ upon deuteration can be accounted for: both the v_{SI}'s and $\Gamma_{\parallel}/\hbar$ tunneling rates are significantly smaller for D_2CO than for H_2CO.

[Note that in the above we have resurrected $\Gamma_{\parallel}$ matrix elements to allow for 10^6–10^7-s^{-1} tunneling rates of the I states. It does *not* follow trivially that diagonalization of the resulting $\boldsymbol{H}_{eff}$ matrix—see eq 1 through 4—will lead to a comparable decay rate for S. Rather it is necessary that the S_1–S_0 coupling energies (i.e., the $\{v_{SI}\}$) be large enough.]

At this point one might conclude that all is well—but we still have not accounted in any way for the observed time lag between S_1 decay and appearance of products.

B. The "Time Lag" and Reaction Intermediates

If the S_1 collisionless decay is induced by tunneling, then H_2 + CO products will obviously appear on the same time scale. Thus it becomes necessary to assert that collisions "quench" the $S_1 \rightsquigarrow H_2 + CO$ tunneling process by bringing the molecule instead to S_0 states which cannot dissociate without further collision. If this $S_1 + M \rightarrow I + M \rightarrow H_2 + CO + M$ quenching process were to occur, for example, at a rate of 10^8 s^{-1}/torr—this is the slope of the low-pressure, linear, $1/\tau_{S_1}$ vs. P Stern–Volmer plot—then the quenching could indeed begin to overtake the collisionless tunneling at pressures of 0.1 torr (the lowest pressure for which the time lag is measured). But it seems unlikely to us that collisions would preferentially quench S_1 into S_0 states which cannot dissociate (unless of course a sufficient amount of energy is removed at the same time).

And how can collisions take these otherwise long-lived states to products at one-sixth gas kinetic rate (see section IIC)? It is conceivable that these collisions are essentially elastic, simply serving to couple the long-lived states with isoenergetic vibrational levels which can tunnel efficiently to products. Along these lines, the possibility of weakly coupled vibrational states ("trapped trajectories"?,[54] "local modes"?[55]) needs to be carefully investigated for the ground potential-energy surface of formaldehyde.

A metastable hydroxymethylene species (HCOH) has recently been established for S_0-H_2CO. Ab initio calculations (ref 4, 56, and references to earlier work contained therein) find a minimum at ~50 kcal/mol on the S_0 surface, corresponding to the HCOH radical. Along the minimum energy pathway to H_2CO it must surmount a barrier of ~45 kcal/mol. Sodeau and Lee[26] have found spectroscopic evidence for HCOH in their matrix-isolation photolysis studies, thereby suggesting its role as intermediate in the time-lagged appearance of H_2 + CO products. But we see no good reason why the hydroxymethylene isomer should be longer lived than any other vibrationally excited formaldehyde ground state. In fact, Miller[53] estimates that—at realistic excitation energies—HCOH tunnels to H_2CO faster than H_2CO tunnels to products.

It has been suggested that HCOH is implicated specifically in the primary $S_1 \rightsquigarrow S_0$ step, that the "internal conversion to S_0* is more probable for the hydroxycarbene rearrangement than for the direct dissociation mechanisms".[56] More explicitly it has been shown that, as the nuclei are displaced from their equilibrium configuration $Q = 0$, the nonadiabatic interaction terms

$$V_I^{10}(Q)/[E_0(Q) - E_1(Q)]$$

increase most dramatically for $Q \neq 0$ corresponding to the $H_2CO \rightarrow$ HCOH rearrangement. But for optical excitation to vibrational levels near the S_1 origin the molecule does not have sufficient energy to get away from its equilibrium configuration—recall that $Q_{S_1}^{eq} \approx Q_{S_0}^{eq}$. Thus the only nonadiabatic couplings relevant to the S_1–S_0 internal conversion are those with $Q \sim Q_{S_1}^{eq} \sim$ "$Q_{H_2CO}^{eq}$" $\neq$ "Q_{HCOH}"; that is, in the Q integration specified in eq 10, only those $Q \approx Q_{H_2CO}^{eq}$ make nonnegligible contributions. Collision might allow HCOH to play more of a role in the S_1–S_0 interaction; the inclusion of a second molecule will modify completely any discussion of the effective potential energy for nuclear motion by changing barrier heights and shapes, etc. Preliminary studies of these collision effects are just now being reported.[57]

Another intermediate which has been invoked is the lowest triplet state T_1; its role has been implicated by magnetic rotation effects in S_0–S_1 absorption,[16] benzene-sensitized dissociation,[24] and O_2- and NO-enhanced product formation.[29] But T_1 is observed[23] to undergo a fast (<100 ns) nonradiative relaxation to S_0, indicating that it cannot provide the "bottleneck" necessary to account for the microsecond time lag. Furthermore, we found earlier (sections IIIA and B) that the unbroadened ($\Gamma_{\parallel} = 0$) S_0 levels are not sufficiently closely spaced to induce a radiationless decay of S_1—the T_1 levels are still sparser. [In this regard it has been suggested that rotational degrees must be explicitly considered and that their proper inclusion would lead to a sufficiently high density of states in S_0. Such an investigation would be extremely valuable, not just for a better understanding of the formaldehyde photophysics but to advance in general the theory of radiationless transitions in intermediate-sized molecules.] The only way in which T_1 could play a dominant role, in fact, is if the $S_1 \rightsquigarrow T_1$ process were *collision-induced* and *inelastic*; then the low density of T_1 levels would be irrelevant and the $T_1 \rightsquigarrow S_0$ relaxation would be slower than 0.01 ns because of the excess-energy removal.

C. Rotation and Electric Field Effects

We have referred earlier to a dramatic dependence on rotational state of the fluorescence lifetimes measured for rovibrational levels near the S_1 origin. Within the zero-point vibrational levels, for example, Weisshaar and and Moore[58] have observed hundredfold fluctuations in fluorescence lifetimes as the rotational quantum numbers J and K are varied. Their experiments were done in a bulb, at pressures in the millitorr range. (The data agree with those obtained by Luntz[37] in a thermal beam, where excitation of specific K states—averaged over many J—in the zero-point level occurs.) On the average, the lifetimes decrease slightly with increasing K or rotational energy, but no other simple or systematic trends are discernible. Recall furthermore that, because H_2CO is not quite a symmetric top, there is a small splitting of the $\pm K$ levels. In all cases for which the two S_1 components (corresponding to a K doublet) could be selectively excited, quite different lifetimes were observed for the two components. For $J' = 6$ and $K' = 3$, the components are split by only 8×10^{-4} cm^{-1} in S_1, but the lifetimes differed by a factor of three!

Selzle and Schlag[36] have also measured fluorescence lifetimes of S_1-formaldehyde as a function of rotational quantum numbers. Their experiments were carried out in a hypersonic jet instead of a low-pressure bulb sample. Under conditions of isoentropic expansion the cooling of the gas eliminates sequence congestion so effectively that the rotational purity of each absorption line is guaranteed. Only contributions to the spectrum from rotational states with $J \leq 5$ are involved. Furthermore, Selzle and Schlag chose to study not the zero-point vibrational level, but instead the $2^2 4^1$ state, i.e., that with two quanta of excitation in the ν_2 (CO stretch) mode and one quantum in ν_4 (out-of-plane "wag"). This vibronic state of S_1 is known to be magnetically sensitive,

indicating its perturbation by T_1 states.[16] They found a small (~30%) variation in the lifetime of individual rotational levels of the $2^2 4^1$ band. In addition, Lee and co-workers have measured fluorescence quantum yields for many rotational levels in the 4^1 (ref 35) and $2^3 4^1$ (ref 25) vibrational bands; in both instances variations by a factor of 2–4 were observed.

The following question must then be confronted. What is the source of the fluctuation in fluorescence lifetime with rotational quantum number? In particular, why is it so much more dramatic in the zero-point and 4^1 bands than in the higher energy $2^2 4^1$ state? And how can it be explained in the case of K doublets whose S_1 splitting is as small as 10^{-3} cm^{-1}?

Consider again the coupling scheme discussed in section IIIA and shown in Figure 2. In general, i.e., for arbitrary v_{SI}'s, Γ_I's, and $(E_S - E_I)$'s, its solution requires large-scale numerical computation and leads to complicated multiexponential decay and damped oscillations. In the special case of weak coupling $[|v_{SI}|^2 \ll (E_S - E_I)^2 + (\Gamma_S - \Gamma_I)^2/4$, for all $I]$, however, it can be shown[59] that $P_S(t)$ decays exponentially with a rate

$$k_S^{nr} = \frac{1}{\hbar} \sum_I \frac{|v_{SI}|^2 \, \Gamma_I}{(E_S - E_I)^2 + \Gamma_I^2/4} \qquad (17)$$

Actual theoretical estimates (see section IIIA) of v_{SI}, $(E_S - E_I)$ and Γ_I confirm that the weak coupling inequality is reasonably satisfied. Furthermore, $\Gamma_S \ll \Gamma_I$, as is also required for the derivation of (17). In any case, it is useful to treat (17) as a qualitatively valid relationship between the observed fluorescence rate and the fundamental molecular parameters. In particular, k_S^{nr} is seen to vary with initial state $|S\rangle$ according to v_{SI} and $E_S - E_I$. Since different I contribute to $\sum_I$ for different $|S\rangle$, there is also an indirect dependence of k_S^{nr} on Γ_I.

More specifically we want to account for the large fluctuations observed in k_S^{nr} as S runs through different rotational levels of a given vibrational band. Recent theoretical work[60,61] suggests that the v_{SI} coupling matrix elements do not depend strongly on the rotational quantum numbers characterizing $|S\rangle$. Instead, the dramatic variation of fluorescence rate k_S^{nr} with $|S\rangle$ arises from the rotational selection rules on v_{SI} which produce a random energy matching of $|S\rangle$ and $|I\rangle$ levels. That is, for certain rotational states $|S\rangle$, the nonzero v_{SI} matrix elements involve $|I\rangle$, states for which $E_S - E_I$ happens to be very small. These "accidental" resonances give rise to the large fluctuations in k_S^{nr}. Recall further that the Γ_I's are small compared to the spacings of $|I\rangle$ levels. Thus a picture emerges according to which each $|S\rangle$ state interacts with a "lumpy" I continuum [formed from the diagonalization of $v_{II'}$ and $v_{I\epsilon}$ in the $\{|I\rangle\} - \{|\epsilon\rangle\}$ basis—see Figure 2 and the effective Hamiltonian discussion of section IIIA]. As we pass from one $|S\rangle$ to another, by preparing the system successively in different rotational levels of a given vibrational band, the $|S\rangle$ state passes into and out of resonance with the "lumps" (E_I's) in the I continuum. As the total energy is increased, k_S^{nr} is expected to increase and to become a smoother function of S, since both v_{SI} and in particular Γ_I are increasing significantly. This is consistent with Selzle and Schlag[36] finding shorter and smoother lifetimes for the $2^2 4^1$ band than Weisshaar and Moore[31] observed for the zero-point and 4^1 levels.

Preliminary attempts to confirm this picture and to extract rough estimates of v_{SI}, Γ_I, and $E_S - E_I$, have come from the recent Stark experiments of Weisshaar and Moore.[38] Essentially what they have done is to repeat their earlier k_S^{nr} measurements for individual rotational levels of 4^1-S_1 formaldehyde, but now in the presence of an external electric field. For field strengths no larger than a few kV/cm, it is easy to show that *inter*electronic Stark effects are altogether negligible compared to the S_1–S_0 matrix elements of the nuclear kinetic energy. Thus v_{SI} is essentially unperturbed by the external electric field. Similarly we do not expect the Γ_I's to be effected, since these widths are associated with either tunneling through a potential energy barrier or with collisional deactivation. Almost certainly the main effect of the Stark field is to "tune" (since S_1- and S_0-H_2CO have different dipole moments) the small energy difference $(E_S - E_I)$ so that $|S\rangle$ is moved into and out of resonance with the lumpy continuum.

Indeed Weisshaar and Moore have found that for $E_S - E_I$ shifts as small as 3×10^{-4} cm^{-1} (i.e., for electric fields as small as 70 V/cm) the fluorescence lifetime of a 4^1-rotational level changes by more than a factor of six. From eq 17 this requires that v_{SI}, Γ_I, and $E_S - E_I$ must all be small. From more careful analyses of an extensive series of measurements on the electric field dependences of k_S^{nr}'s, Weisshaar and Moore conclude that v_{SI} and Γ_I are on the order of 10^{-3} cm^{-1} and that $E_S - E_I$ is ~10^{-2}–10^{-3} cm^{-1}. These values are all consistent with the ab initio theoretical estimates discussed in section III. Clearly it will be useful to pursue further Stark studies of H_2CO fluorescences, particularly those which will involve Doppler-free excitation of single J, K, M levels in S_1.

D. Summary, and More Open Questions

In the above review we have neglected to discuss a large amount of experimental data obtained recently on the spectroscopy and photophysics of the formaldehyde molecule. Some of these measurements were at least mentioned in the Introduction (section I). But many of them, including in particular the collisional studies of Moore and co-workers and the fluorescence quantum yield determinations of Lee et al., have been essentially suppressed altogether. (Discussions of these important works can be found in the doctoral thesis of Weisshaar and in the recent review by Lee and Loper[45] and in the many references to original papers cited therein.) We have so "streamlined" this present review with the purpose of focussing more clearly on the basic problem of reconciling the fast, collisionless nonradiative decay of S_1-H_2CO with the time lag observed at higher pressures for appearance of products. This problem forces us to confront squarely several fundamental difficulties in our understanding of radiationless electronic relaxation and of indirect photodissociation in small polyatomic molecules.

First, is formaldehyde large enough to show nonradiative decay of its S_1 state in the absence of collision or dissociation? The low-pressure bulb and molecular beam experiments described earlier confirm certainly that S_1-nonradiative decay is present in the collision-free limit. But no laboratory measurement to date has succeeded in searching unambiguously for dissociation products in this same zero-pressure limit. Accordingly, theory has stepped in—see section III—and concluded tentatively that nonradiative decay of the excited electronic state is not possible without the (virtually) simultaneous dissociation of the molecule on its ground-state surface. These predictions are based on estimates of the S_1–S_0 coupling energies ($\{v_{SI}\}$) and on the S_0 density of states in the region of the S_1 origin.

The various calculations of the S_1–S_0 v_{SI}'s, described in sections IIIA,B, have involved quite different theoretical approximations, e.g., Herzberg–Teller expansion vs. separable representations of the electronic couplings and quadratic vs. diagonally anharmonic approximations for the potential-energy surfaces. But the final estimates of v_{SI} magnitudes and their dramatic variations with I have shown qualitative agreement and represent reasonable upper bounds on the true behavior. [Larger values of v_{SI} would necessarily imply new anomalies in the S_0–S_1 absorption which would be inconsistent with presently accepted deperturbation analyses of the high-resolution spectra.] The density-of-states estimates, on the other hand, are somewhat more problematic.

For the most part, the spacing of vibrational levels in polyatomic molecules has been described within an assumption of harmonicity. Then the density of states at an arbitrary total

vibrational energy follows directly from combinatoric relations, evaluated for the known normal mode frequencies and degeneracies.[62] Keeping the modes separable but allowing for anharmonicity in each mode lead to an enhancement of the vibrational density only if the number of modes or the total energy is large enough. van Dijk et al. have found, for example, using one-dimensional cross-sections ("slices") of their ab initio surfaces, that the separable S_0 density at $E = E_{S_1}$ is enhanced very little over what it would be if the single-mode potentials were assumed harmonic for all displacements (rather than only at $Q_i \sim 0$). Furthermore, taking into account the "off-diagonal" (*non*separable) anharmonicity implicit in the S_0 surface of Morokuma et al., Elert et al. have derived a level spacing near E_{S_1} which is again comparable with van Dijk et al.'s. The density of S_0 vibrational levels in this region is almost certainly no greater than 10–20 per cm^{-1}.

Suppose we try to "improve" the situation by including the rotational degrees of freedom. Whereas the total angular momentum J is assuredly a good quantum number, there are many reasons to believe that K is significantly "degraded". In particular, both coriolis coupling and deviations from symmetric-top symmetry will serve to mix K states. Due to these effects the density of coupled rovibronic levels in S_0 can be increased by *at most* a factor of $(2J + 1)$. On the average only one-fourth of these will have the right symmetry to interact with $|S\rangle$. Thus the *maximum* density of S_0 levels is $(2J + 1)\rho/4$, where ρ is the purely vibrational value discussed above. For $J \sim 10$–20, we have then an enhancement factor of only 5–10. This still leaves the effective density of states far too low for v_{SI}'s on the order of 10^{-3} cm^{-1} to result in fast (100 ns) intramolecular radiationless decay. Our prediction stands that the observed zero-pressure S_1 fluorescences require simultaneous dissociations on the ground-state surface.

But how then can the time lag observed at higher pressures be explained? In section IVB we have already reviewed this question. Basically the idea is that the prompt intramolecular S_1-$H_2CO \rightsquigarrow H_2 + CO$ reaction is quenched by collision. That is, the two-step mechanism S_1-$H_2CO + M \rightarrow I + M \rightarrow H_2 + CO + M$ becomes dominant, with the second step corresponding to the slow process monitored in the Houston-Moore and Zughul experiments. Three candidates—vibrationally hot S_0, the hydroxymethylene isomer, and the triplet T_1—were discussed earlier as possible (but unlikely!) intermediates I. Certainly some complicated combination of all three effects is involved. T_1 admixture in both the S_1 and isoenergetic S_0 levels can account for the O_2 and NO enhancement of product yield, the unusual D_2CO quenching behavior, the S_0–S_1 magnetic rotation activity, and the benzene sensitization. In turn, the presence of a deep HCOH minimum in the ground-state surface suggests the importance of "off-diagonal" (nonseparable) anharmonicity on the vibrational structure and dynamics. Finally, many "hot" S_0 states will in general not correspond to a proper distribution of vibrational energy for dissociation to take place—collisions are necessary to "nudge" them into a reactive form, or, as mentioned at the start (and end) of section IVB, "hot" S_0 (and T_1) might be formed from S_1—via inelastic collisions—with low enough energy ($< E_{S_1}$) to remain intact as long as it stays isolated.

In this connection it is significant that realistic nonseparable potential-energy surfaces which include as good a description of the dissociation limits as of the spectroscopically accessible minima, are only now becoming available. Murrell and coworkers[63] have recently suggested simple analytical forms for empirical surfaces of this kind for a wide variety of three- and four-atom molecules including formaldehyde. Clearly it is most essential that these results be used to probe theoretically the dynamics of vibrational energy redistribution and unimolecular reaction.

On the experimental side, the key lesson learned is that measurements must be carried out at surprisingly low pressures before collision-free information can be deduced. Now that "zero-pressure" S_1 fluorescence lifetimes are available it is imperative that comparably unambiguous experiments be completed on the search for S_0 dissociation products. Only in this way will the true role of collisions, dimers, and vibrationally "hot" intermediates become understood.

Table V. Herzberg-Teller Coefficients for H_2CO and D_2CO[a]

		First Order $R(i;j)$	[amu-Å^2]$^{-1}$
i	j	H_2CO	D_2CO
4	5	3.119	5.573
4	6	−4.069	−5.358
5	4	7.898	14.074
6	4	−10.309	−13.572

			Second Order $R(i;j,k)$	[amu-Å^2]$^{-3/2}$
i	j	k	H_2CO	D_2CO
1	4	5	−45.33	−33.615
1	4	6	59.44	32.438
2	4	5	−61.02	−128.350
2	4	6	79.66	122.010
3	4	5	−34.43	−43.561
3	4	6	44.94	42.040
4	1	5	−63.33	−45.359
4	1	6	80.83	43.765
4	2	5	−86.91	−182.050
4	2	6	113.40	175.650
4	3	5	−48.53	−60.404
4	3	6	63.34	58.284
5	1	4	−0.0132	−0.0167
5	2	4	−0.0087	−0.0112
5	3	4	−0.0057	−0.0049
6	1	4	0.0031	0.0023
6	2	4	0.0020	0.0016
6	3	4	0.0013	0.0007

[a] The first- and second- order Herzberg-Teller coefficients, $R(i;j)$ and $R(i;j,k)$, are defined by eq A3 and A7 in Appendix A.

Table VI. S_1-S_0 Geometry Shifts for Normal Modes[a]

	H_2CO		D_2CO	
mode	Δ [amu$^{1/2}$-Å]	δ	Δ [amu$^{1/2}$-Å]	δ
1	−0.028	−0.254	−0.095	−0.742
2	0.278	2.002	0.284	2.016
3	0.147	0.980	0.104	0.596
4	0	0	0	0
5	0	0	0	0
6	0	0	0	0

[a] $\Delta = Q' - Q$ is the change in equilibrium value of the (mass-weighted) normal coordinate upon passing from S_1 to S_0; $\delta = (\omega'/\hbar)^{1/2}\Delta$ is the corresponding *dimensionless* geometry change. (The primed quantities refer to S_0.)

Acknowledgments. We are grateful to James Weisshaar for communicating to us his unpublished work with Bradley Moore and for many very helpful conversations. Similarly we are grateful to William Miller, Fritz Schaefer, and John Goddard for discussion of their tunnelling and electronic structure calculations. Many talks over the years with Michael Berry, Karl Freed, Eric Heller, Sydney Leach, Ed Lee, Alan Luntz, Bradley Moore, Stuart Rice, and James Yardley have also contributed to our better understanding of the molecular photodissociation process.

V. Appendixes

A. Herzberg–Teller Calculations

Consider the nonadiabatic coupling term displayed in (9) and recall that $\psi_{S_0}(qQ)$ and $\psi_{S_1}(qQ)$ are the first two eigenfunctions of $H_{el}(qQ) \equiv T(q) + V(qQ) \equiv H_{total} - T(Q)$. Herzberg–Teller theory amounts to Taylor series expanding $H_{el}(qQ)$ about some Q_0 and treating the Q-dependent terms as a perturbation, V. We write

$$V \equiv H_{el}(qQ) - H_{el}(qQ_0) = \sum_l \left(\frac{\partial H_{el}}{\partial Q_l}\right)_{Q_0} (Q_l - Q_l^0) + \frac{1}{2}\sum_l\sum_j \left(\frac{\partial^2 H_{el}}{\partial Q_l \partial Q_j}\right)_{Q_0} (Q_l - Q_l^0)(Q_j - Q_j^0) + \ldots \quad \text{(A1)}$$

Henceforth we shall put $Q_l^0 = 0$, so that $Q_l - Q_l^0 \rightarrow Q_l$, etc. Solving for $\psi_{S_0}(qQ)$ and $\psi_{S_1}(qQ)$ through second order in the normal mode displacements $\{Q_l\}$, we obtain the following result for the electronic matrix element:

$$\left\langle \psi_{S_1}(qQ)\left|\frac{\partial}{\partial Q_l}\right|\psi_{S_0}(qQ)\right\rangle_q = D_{S_0}^{S_1}(l) + \sum_j [D_{S_0}^{S_1}(lj) + \sum_{n\neq 0,1} D_{S_1}^{S_n}(j) D_{S_0}^{S_n}(l)] Q_j + \sum_j\sum_k \left[\sum_{n\neq 1} D_{S_1}^{S_n}(j) D_{S_0}^{S_n}(jk) + \frac{1}{2}\sum_{n\neq 0} D_{S_0}^{S_n}(l)\, D_{S_1}^{S_n}(jk)\right] Q_j Q_k \quad \text{(A2)}$$

Here

$$D_{S_m}^{S_n}(l) \equiv \left\langle \psi_{S_n}(q0)\left|\left(\frac{\partial U}{\partial Q_l}\right)_0\right|\psi_{S_m}(q0)\right\rangle_q / [E_m(0) - E_n(0)] \equiv V_l^{nm}(0)/[E_m(0) - E_n(0)] \quad \text{(A3)}$$

Also,

$$D_{S_m}^{S_n}(lj) = -\sum_{n\neq m} D_{S_m}^{S_n}(l) D_{S_m}^{S_n}(j) \quad \text{(A4)}$$

and, for $m \neq n$, eq A5 holds.

$D_{S_n}^{S_m}(l)$ and $D_{S_n}^{S_m}(lj)$ are the first- and second-order (with respect to the normal mode displacements) coefficients which express each $\psi_{S_n}(qQ)$ as a linear combination of the $\psi_{S_m}(q0)$'s:

$$\psi_{S_n}(qQ) = \psi_{S_n}(q0) + \sum_{m\neq n}\sum_l D_{S_n}^{S_m}(l) Q_l \psi_{S_m}(q0) + \frac{1}{2}\sum_m\sum_l\sum_j D_{S_n}^{S_m}(lj) Q_l Q_j \psi_{S_m}(q0) + \theta(Q^3) \quad \text{(A6)}$$

In our actual calculations of the expansion coefficients, the choice of zero-order geometry Q_0 is limited by the availability of ab initio results for the corresponding $\{\psi_{S_m}(qQ_0)\}$. Thus, although recent work[8] has required the $\{Q_l^0\}$ to optimize the convergence of Herzberg–Teller series, we confine ourselves to the choice $Q_0 = Q_{eq}^{S_0}$. In addition to the availability of suitable wave functions,[5] this choice allows maximum use of symmetry arguments in eliminating contributions to $\langle\psi_{S_1}(qQ)|(\partial/\partial Q_l)|\psi_{S_0}(qQ)\rangle$. Specifically, $\langle\psi_{S_n}(qQ)|(\partial U/\partial Q_l)_0|\psi_{S_m}(qQ)\rangle_q$ and hence $D_{S_n}^{S_m}(l)$ vanish unless the representation of the direct product $\psi_{S_n}(qQ) \otimes \psi_{S_m}(qQ)$ contains the representation of Q_l. [The "q" symmetry of $(\partial U/\partial Q_l)_0$ is the same as the "Q" symmetry of Q_l.] Table II lists the symmetry species and energies of the normal modes $\{Q_l\}$ and of the zero-order electronic wave functions $\{\psi_{S_m}(qQ)\}$ appropriate to formaldehyde. Only the five lowest singlets are included, since large energy denominators in $D_{S_0}^{S_m}$ or $_{S_1}(l)$ and $D_{S_0}^{S_m}$ or $_{S_1}(lj)$ make unnecessary the inclusion of higher states. Note that the vertical excitation energies appearing in the last column of Table IIB are precisely the $\{E_m(0)\}$ needed in the Herzberg–Teller coefficients.

When the electronic matrix element in eq (A2) is rewritten as

$$\left\langle \psi_{S_1}(qQ)\left|\frac{\partial}{\partial Q_l}\right|\psi_{S_0}(qQ)\right\rangle_q = D_{S_0}^{S_1}(l) + \sum_j R_{S_0}^{S_1}(l;j) Q_j + \sum_j\sum_k R_{S_0}^{S_1}(l;jk) Q_j Q_k \quad \text{(A7)}$$

and the basis set of Table IIB is used, the following nonzero coefficients are obtained for the Herzberg–Teller expansion in formaldehyde.

First order

$$R_{S_0}^{S_1}(4;\tfrac{5}{6}) = D_{S_0}^{S_1}(4,\tfrac{5}{6}) + D_{S_1}^{S_2}(4) D_{S_0}^{S_2}(\tfrac{5}{6})$$

$$R_{S_0}^{S_1}(\tfrac{5}{6};4) = D_{S_0}^{S_1}(4,\tfrac{5}{6}) + D_{S_1}^{S_4}(\tfrac{5}{6})\, D_{S_0}^{S_4}(4) \quad \text{(A8)}$$

Second Order

$$R_{S_0}^{S_1}(l;4,\tfrac{5}{6}) = D_{S_0}^{S_4}(4) D_{S_1}^{S_4}(l,\tfrac{5}{6}) + D_{S_0}^{S_2}(\tfrac{5}{6})\, D_{S_1}^{S_2}(l,4)$$

$$R_{S_0}^{S_1}(4;l,\tfrac{5}{6}) = D_{S_0}^{S_3}(l) D_{S_1}^{S_3}(4,\tfrac{5}{6}) + D_{S_0}^{S_2}(\tfrac{5}{6}) D_{S_1}^{S_2}(l,4) + D_{S_1}^{S_2}(4)\, D_{S_0}^{S_2}(l,\tfrac{5}{6})$$

$$R_{S_0}^{S_1}(\tfrac{5}{6};l,4) = D_{S_0}^{S_3}(l)\, D_{S_1}^{S_3}(4,\tfrac{5}{6}) + D_{S_0}^{S_4}(4)\, D_{S_1}^{S_4}(l,\tfrac{5}{6}) + D_{S_1}^{S_4}(\tfrac{5}{6})\, D_{S_0}^{S_4}(l,4) \quad \text{(A9)}$$

The forms of the *first*-order Herzberg–Teller coefficients $R_{S_0}^{S_1}(l,j)$ have been given previously by Yeung and Moore;[27] they treated the expansion coefficients as adjustable parameters, using the form of (A8) only to determine vibrational selection rules for the corresponding Franck–Condon factors. Since we wish to provide estimates of the electronic factors, we include as well the second-order coefficients in order to check the convergence of the expansion.

Note that

$$\frac{\partial U}{\partial Q_l} = -\frac{\partial}{\partial Q_l}\sum_e\sum_n \frac{Z_n e^2}{r_{en}} = \sum_e\sum_n \frac{Z_n e^2}{r_{en}^2}\left(\frac{\partial r_{en}}{\partial Q_l}\right) \quad \text{(A10)}$$

where, as in the text, Z_n is the charge on the nth nucleus and r_{en} is the distance between nucleus n and electron e. [The term $\sum\sum Z_n Z_{n'} e^2/r_{nn'}$ in U also depends on Q of course, but it cannot contribute to the electronic state coupling since it is q independent.] For small nuclear displacements, $(\partial r_{en}/\partial Q_l) = \hat{r}_{en}\cdot(\partial \mathbf{S}^n/\partial Q_l)$, where again as in section III $\mathbf{S}^n$ is the vector position of the n nucleus. It then follows that

$$\left\langle \psi_\gamma(q0)\left|\left(\frac{\partial U}{\partial Q_l}\right)_0\right|\psi_\lambda(q0)\right\rangle_q = e^2\sum_n \left(\frac{\partial \mathbf{S}^n}{\partial Q_l}\right)_0 Z_n \left\langle \psi_\gamma(q0)\left|\sum_e \left(\frac{\mathbf{r}_{en}}{r_{en}^3}\right)_0\right|\psi_\lambda(q0)\right\rangle \quad \text{(A11)}$$

as written in eq 14 (there we have written $\mathbf{q}^e - \mathbf{S}^n$ for $\mathbf{r}_{en}$ and written out the scalar product in terms of the Cartesian components). This form for $V_l^{\gamma\lambda}(0)$ was first given by Murrell and Pople[64] and used shortly thereafter by Pople and Sidman[10] to

$$D_{S_n}^{S_m}(lj) = \frac{\left\{\left\langle \psi_{S_m}(q0)\left|\left(\frac{\partial^2 U}{\partial Q_l \partial Q_j}\right)_0\right|\psi_{S_n}(q0)\right\rangle_q - V_l^{nn}(0) D_{S_n}^{S_m}(j) - V_j^{nn}(0) D_{S_n}^{S_m}(l) + \sum_{p\neq n}[V_l^{mp}(0) D_{S_n}^{S_p}(j) + V_j^{mp}(0) D_{S_n}^{S_p}(l)]\right\}}{E_n(0) - E_m(0)} \quad \text{(A5)}$$

estimate the intensities in the Herzberg–Teller-allowed $S_0 \rightarrow S_1$ absorption spectrum of formaldehyde. Since $\sum_e(r_{en}/r_{en}^3)$ is a sum of one-electron operators, its matrix elements are particularly amenable to computation. Also, the $\partial \mathbf{S}^n/\partial Q_l$ are "simply" the transformation coefficients between Cartesian and normal coordinates, and thus follow directly from a normal mode analysis.

[From eq A5 for the *second*-order coefficients $D_{S_n}^{Sm}(ij)$ it would appear that we need also to consider the matrix elements of the *second* partial derivatives of U. But it can be shown[40] that—for small nuclear displacements—the relevant $\langle\psi_\gamma(q0)|(\partial^2 U/\partial Q_i \partial Q_j)_0|\psi_\lambda(q0)\rangle$'s vanish identically.]

$$\langle\psi_\gamma(q0)|(\partial^2 U/\partial Q_i \partial Q_j)_0|\psi_2(q0)\rangle\text{'s}$$

The electronic wavefunctions required to evaluate matrix elements of the one-electron operator $\sum_e(r_{en}/r_{en}^3)_0$ are generated from $\psi_{S_0}(q0)$ by promoting one or more electrons into the appropriate virtual orbitals. This approximate description of the higher lying singlets is necessary since accurate ab initio wavefunctions are available only for S_0 and S_1. The explicit form of the off-diagonal matrix elements of a one-electron operator $\theta \equiv \sum_e \theta(e)$ between a closed-shell ground-state singlet, $^1\psi_0$, and a corresponding, singly excited open-shell singlet, $^1\psi_1$, is well-known (see, for example, the discussion in ref 40). If $^1\psi_1$ is the state which arises from $^1\psi_0$ by promotion of an electron from an occupied orbital ϕ_n to a virtual orbital ϕ_{n+1}, then $\langle {}^1\psi_0|\theta|{}^1\psi_1\rangle = 2^{1/2}\langle\phi_n(e)|\theta(e)|\phi_{n+1}(e)\rangle$. In the case of *two* open-shell singlets, $^1\psi_1$ and $^1\psi_2$, we have similarly that $\langle {}^1\psi_1|\theta|{}^1\psi_2\rangle = \pm\langle\phi_k(e)|\theta(e)|\phi_l(e)\rangle$ where ϕ_k and ϕ_l are the unmatched molecular orbitals.

The electronic matrix elements may be further reduced by considering the LCAO approximation for the relevant molecular orbitals. If

$$\phi_\eta = \sum_n \sum_\alpha a_{\alpha\eta}\lambda_n{}^\alpha \tag{A12}$$

where $\lambda_n{}^\alpha$ is an atomic orbital of type α (1s,2p, etc.) centered on nucleus n, then

$$\langle\phi_\eta|\theta(e)|\phi_\mu\rangle = \sum_n \sum_{n'} \sum_\alpha \sum_{\alpha'} a_{\alpha\eta} a_{\alpha'\mu}$$

$$\langle\lambda_n{}^\alpha(\theta(e)|\gamma_{n'}{}^{\alpha'}\rangle \sim\approx \sum_{n'} \sum_\alpha \sum_{\alpha'} a_{\alpha\eta}\, a_{\alpha'\mu}\, \langle\lambda_{n'}{}^\alpha|\theta(e)|\lambda_{n'}{}^{\alpha'}\rangle \tag{A13}$$

Here we have assumed (CNDO approximation) that the overlap of two atomic orbitals on different nuclei ($n \neq n'$) can be neglected. Thus the integrals $\langle\psi_\gamma|\sum_e(r_{en}/r_{en}^3)_0|\psi_\lambda\rangle$ required for evaluation of the nonadiabatic interactions can be reduced to a sum of one-electron integrals of the form $\langle\lambda_{n'}{}^\alpha|(r_{en}/r_{en}^3)_0|\lambda_{n'}{}^{\alpha'}\rangle$, where n and n' denote two different atomic centers. The necessary LCAO's are taken from the ab initio ground-state wave function of Aung, Pitzer, and Chan;[5] the required excited states are generated by promotion of appropriate into virtual orbitals as mentioned above. To complete our evaluation of the electronic factor (see eq A11) it remains only to treat the derivatives $(\partial \mathbf{S}^n/\partial Q_l)_0$. As noted earlier these derivatives are simply the coefficients of the linear transformation between Cartesian displacements and normal coordinates Q; we have used the normal-mode analysis of Duncan and Mallison.[65] Due to differences in normal-mode characteristics for the two isotopes, the resulting Herzberg–Teller coefficients are also different (see Table V).

No estimates of the coefficients listed in Table V have been reported elsewhere. However, a few of the $D_{S_n}{}^{S_m}(i)$ factors which appear in the first-order coefficients have been calculated by Pople and Sidman.[10] Actually, they reported only the quantities $(\overline{Q_i^2})^{1/2}\,[E_m(0) - E_n(0)]D_{Sm}{}^{Sn}(I)$, from which the $D_{Sm}{}^{Sn}(i)$ can be extracted using Hendersen's[9] electronic energy differences (see Table IIB) and the relation $\overline{Q_i^2} = \hbar/2\nu_i$ (with vibrational frequencies from Table IIA). In this way we find values of −3.0, −0.2, and −0.1 amu$^{-1/2}$ Å^{-1} for $D_{S_1}{}^{S_2}(4)_1, D_{S_2}{}^{S_4}(5)$, and $D_{S_2}{}^{S_4}(6)$, compared to our own estimates of −4.1, −0.16, and −0.04 amu$^{-1/2}$ Å^{-1}. Considering the difference between these two studies, the agreement is surprisingly good. In Appendix B we find further that the Herzberg–Teller wave functions calculated here (see eq A7) give rise to interaction energies v_{SI} which agree quite well with those obtained by van Dijk et al., who have specifically avoided the Herzberg–Teller expansion.

B. Evaluation of Coupling Matrix Elements

From Appendix A, the general form of the coupling matrix element between the two vibronic levels $S_1 v$ and $S_0 w$ can be written through second-order in the Herzberg–Teller expansion as

$$\langle\Psi_{S_0 v}(qQ)|H|\Psi_{S_1 w}(qQ) =$$
$$-\hbar^2 \sum_l \left\{ \left\langle \chi_{S_0 v}(Q)\left|\frac{\partial}{\partial Q_l}\right|\chi_{S_1 w}(Q)\right\rangle_Q \times R_{S_1}{}^{S_0}(i) + \sum_j \left\langle \chi_{S_0 v}|Q_j\frac{\partial}{\partial Q_l}\right|\chi_{S_1 w}\right\rangle R_{S_1}{}^{S_0}(ij) + \sum_j\sum_k \left\langle \chi_{S_0 v}|Q_j Q_k\frac{\partial}{\partial Q_l}\right|\chi_{S_1 w}\right\rangle R_{S_1}{}^{S_0}(i;jk)\right\} \tag{A14}$$

Each vibrational wave function $\chi(Q)$ is the product of six one-dimensional functions, each corresponding to a different normal mode of formaldehyde. Each one-dimensional function is a simple harmonic oscillator eigensolution [or *sum* of them, in the case of the out-of-plane bend (ν_4) of S_1] with the appropriate experimentally determined frequency. The only exception is when χ corresponds to a distribution of vibrational quanta in which $E_{\nu_3} > D$. Then the one-dimensional function associated with ν_3 must be written as the $(E_{\nu_3} - D)$-continuum *Morse*-oscillator solution.

Consider first the case of bound state $\chi_{S_0 w}$'s. Then the Q integrals in eq A14 reduce to matrix elements of $\partial/\partial Q_l$, $Q_j\partial/\partial Q_l$ or $Q_j Q_k \partial/\partial Q_l$ between $\chi(Q)$'s each of which factors into a product of six one-dimensional harmonic oscillator eigenfunctions. The evaluation of these integrals thus involves only the computation of one-dimensional integrals which have Q_l or $\partial/\partial Q_l$ sandwiched between two geometry- and frequency-shifted harmonic oscillator functions. Instead of the (mass-weighted) normal coordinate Q, it is convenient to express everything in terms of the dimensionless $\eta \equiv (\omega/\hbar)^{1/2}Q$, where ω is the angular frequency associated with the mode Q. Similarly, for the geometry- and frequency-shifted oscillator in the second electronic state we put $\eta' = (\omega'/\hbar)^{1/2}Q'$. It is easily shown that η and η' are related by the expression $\eta' = \alpha\eta + \delta$, where $\alpha \equiv (\omega'/\omega)^{1/2}$ and $\delta \equiv (\omega'/\hbar)^{1/2}\Delta$; $\Delta \equiv Q' - Q$, the geometry shift associated with the normal mode upon passing from S_1 to S_0. The values of Δ and δ for each vibration for the S_1–S_0 transition in formaldehyde are given in Table VI. These values are determined from the equilibrium geometries of Table IA, the internal coordinates of Table IB, and normal mode frequencies of Table IIA. [Note that Δ for the out-of-plane bending mode is listed as zero in Table VI, even though the equilibrium geometry of S_1 is nonplanar. This is because the double minimum S_1 function has been expressed in terms of a sum of harmonic oscillators centered at $\theta = 0$.]

By use of the generating function for the Hermite polynomials, all of the one-dimensional overlap integrals and matrix elements of Q and $\partial/\partial Q$ can be evaluated analytically. This was presented in the literature first by Hutchinson[66] and most recently by Yeung,[67] but their published equations contain minor errors. The latest—and hopefully correct—expressions for these integrals are given in reference 40; these are the ones we used to calculated all of the vibrational overlaps and Q, $\partial/\partial Q$ matrix elements appearing in eq A14. Note that in the second-order

terms the possibility of $Q_i = Q_j$ is excluded by symmetry so that the matrix elements of Q^2 do not arise in the case of formaldehyde.

Table III lists our calculated values of v_{sl} for a large number of l states, $\{\chi_{S_0 w}\}$. The distribution **w** of vibrational quantum numbers for each l state is given in the second column. Its "shifted" energy, i.e., the expectation value of the *full* molecular Hamiltonian H with respect to the *harmonic* function $\chi_{S_0 w}$, is given in the third column.

Consider now the *off*-diagonal matrix elements of $V_{S_0}^{anh}(Q)$ between the (S_0) l states. Since we are concerned with S_0 states excited with as much as 30 000 cm^{-1} in vibrational energy, the relevant information about $V_{S_0}^{anh}(Q)$ cannot be derived from the usual infrared spectra analysis but must come instead from a full calculation of the potential-energy surface for large nuclear displacements.

K. Morokuma has kindly provided us with an unpublished analytic fit to the numerical results of his ab initio computations[2] which were carried out to determine the barrier heights and saddle point geometries for dissociation to both radical and molecular products. The potential energy is expressed as the sum of Morse potentials for the C–H, C–O, and "H–H" stretches, plus a term for the double-minimum bending potential of HCO (where the two C–H bond lengths are different), a harmonic out-of-plane bending potential, and assorted correction terms. Scaling factors are used to "turn on" some of the terms in appropriate regions, and each pair of Morse potential parameters are themselves functions of the other bond lengths and angles. The overall surface is fit to the observed force constants and equilibrium geometries for the H_2CO, H + HCO, and H_2 + CO limits. The remaining parameters and correction terms are used to match the calculated barrier heights and saddle point geometries.

Since each term in the above potential involves several bond lengths and angles, all of the normal modes of vibration are effectively coupled to one another. The numerical difficulties of calculating matrix elements of such a potential-energy surface are severe. The terms in $V_{S_0}^{anh}(Q)$ generally *cannot* be written as products of factors, each depending on only one or a few normal coordinates. Since all of the matrix elements have to be evaluated numerically, the integrations become excessively time-consuming when there are more than three dimensions, particularly in the case of unbound $\chi_{S_0 w}$'s where continuum solutions to the Morse potential are involved. To simplify matters, then, $V_{S_0}^{anh}(Q)$ is rewritten as a function of the symmetry coordinates (Table IB). This gives rise to coupling terms the highest dimensionality of which is three. A further transformation to normal coordinates could then be made, but the resulting function has many terms which are five-dimensional. Matrix elements of such terms are impossible to evaluate numerically when a continuum wave function is involved. Thus we have retained the symmetry coordinate representation of $V_{S_0}^{anh}(Q)$. Expressing the basis states as products of one-dimensional symmetry coordinate wave functions for the purpose of computing matrix elements of $V_{S_0}^{anh}(Q)$ is not consistent with the use of normal coordinates elsewhere. However, the matrix elements obtained in this way are expected to be more realistic than those which would be calculated from a less accurate model potential. Table IV shows our results for the $v_{ll'}$'s. Details of the computation of the bound-continuum matrix elements, $v_{S\epsilon}$ and $\{v_{l\epsilon}\}$, are given in ref 40.

C. Convergence Criteria for $|l\rangle$ Basis

By use of the methods described above, it is possible to construct—for any vibrational level of S_1—an effective Hamiltonian matrix whose eigenvalues and eigenvectors give the dynamics of the photodissociation process. In practice, the number of bound S_0 states which interact with an initially prepared S_1 level is so large that computation of the required matrix elements (especially the Γ's) is an excessively difficult task. Furthermore, the resulting H_{eff} matrix would be much too large for machine diagonalization. In this section we outline the selection criteria used to reduce the effective Hamiltonian matrix to diagonalizable size.

In the energy region of interest ($E \sim E_{S_1}$) there are about ten harmonic bound-S_0 levels per cm^{-1}. Approximately one out of four of these states interact with S_1 when nuclear kinetic energy coupling is considered through second order in Herzberg–Teller theory. In addition, S_0 levels which do not directly couple to S_1 do so indirectly by interacting (through $V_{S_0}^{anh}(Q)$) with other S_0 levels which are in turn coupled (via $T(Q)$) to S_1. The S_0 levels which mix one way or another with S_1 contribute to the photodissociation dynamics according to the magnitude of their "widths". From considerable "playing" with the potential basis set, we have arrived at the following criteria for selecting the states which contribute significantly to the photodissociation dynamics.

(i) Consider all harmonic bound-S_0 states which lie within 4000 cm^{-1} of the initial S_1 state (E_{S_1}), calculate the diagonal matrix element of $V_{S_0}^{anh}(Q)$ for each, and retain the 2000 among them whose shifted energies lie closet to E_{S_1}. (Some of these shifts will be as large as thousands of cm^{-1}.)

(ii) Calculate the real part of the H_{eff} matrix element between the S_1 state and each of the 2000 S_0 states retained in (i). Discard any S_0 state whose coupling to the initial S_1 level is more than ten times smaller than $|E_{S_1} - \langle \chi_{S_0 w}| V_{S_0}^{anh}(Q)|\chi_{S_0 w}\rangle|$, the energy difference between the two states.

(iii) Check each state retained in (ii) to determine whether any discarded S_0 levels couple to it with an interaction $(\langle X_{S_0 w}^{retained}| V_{S_0}^{anh}(Q)|X_{S_0 w'}^{discarded}\rangle)$ which exceeds one-tenth their spacing $(|\langle \chi_{S_0 w}^{ret}| V_{S_0}^{anh}|\chi_{S_0 w}^{ret}\rangle - \langle X_{S_0 w'}^{dis}| V_{S_0}^{anh}|X_{S_0 w'}^{dis}\rangle|)$. Reinstate all such $S_0 w'$ levels.

(iv) Calculate all bound-continuum matrix elements of $V_{S_0}^{anh}(Q)$ for each S_0 level which couples directly to S_1 and construct the damping matrix for this set of states. Reinstate all those $S_0 w''$ levels which (although dropped in (ii) and not revived in (iii)) have diagonal Γ's larger than 10^{-5} times $|\langle X_{S_0 w''}| V_{S_0}^{anh}|X_{S_0 w''}\rangle - E_{S1}|$.

By retaining only those S_0 states (generated in (i)) which survive (ii) or which are reinstated by (iii) or (iv), it is estimated that the probability function $P_{S_1}(t)$ differs by less than 3% at any time from what its value would be if more states were included. The most severe restriction in the state selection procedure is the limitation in step i. The cutoff at 2000 states in (i) corresponds to an energy range of ±80 cm^{-1} in H_2CO and ±30 cm^{-1} in D_2CO; the average $S_1 - S_0^{bound}$ coupling energy is orders of magnitude smaller than 30–80 cm^{-1}. The cutoff arises because of the enormous amount of computer time necessary to calculate the bound continuum matrix elements in step iv. This number is proportional to the number of continua available at the initial state energy as well as to the number of states retained in step i.

VI. References

(1) See, for example, S. A. Rice in "Excited States", Vol. 2, E. C. Lim, Ed., Academic Press, New York, 1975, p 111; W. M. Gelbart, *Annu. Rev. Phys. Chem.*, **26**, 323 (1977).
(2) D. M. Hayes and K. Morokuma, *Chem. Phys. Lett.*, **12**, 539 (1972); R. L. Jaffe, D. M. Hayes, and K. Morokuma, *J. Chem. Phys.*, **60**, 5108 (1974); R. L. Jaffe and K. Morokuma, *ibid.*, **64**, 4881 (1976).
(3) J. M. F. van Dijk, M. J. H. Kemper, J. H. M. Kerp, and H. M. Buck, *J. Chem. Phys.*, **69**, 2453 (1978).
(4) J. Goddard and H. F. Schaefer III, *J. Chem. Phys.*, in press.
(5) S. Aung, R. M. Pitzer, and S. I. Chan, *J. Chem. Phys.*, **45**, 3457 (1966).
(6) T. H. Dunning, N. W. Winter, and V. McKoy, *J. Chem. Phys.*, **49**, 4128 (1969); D. B. Neumann and J. W. Moskowitz, *ibid.*, **50**, 2216 (1969).
(7) B. J. Garrison, H. F. Schaefer III, and W. A. Lester, Jr., *J. Chem. Phys.*, **61**, 3039 (1974).
(8) W. Curtis Johnson, Jr., *J. Chem. Phys.*, **63**, 2144 (1975); M. Roche and H. H. Jaffe, *ibid.*, **60**, 1193 (1974).
(9) J. R. Henderson, *J. Chem. Phys.*, **44**, 3496 (1966).
(10) J. A. Pople and J. W. Sidman, *J. Chem. Phys.*, **27**, 1270 (1957).

(11) S. H. Lin, *Proc. R. Soc. London, Ser. A*, **352**, 57 (1976).
(12) J. M. F. van Dijk, M. J. H. Kemper, J. H. M. Kerp, and H. M. Buck, *J. Chem. Phys.*, **69**, 2462 (1978).
(13) V. Sethuraman, V. A. Job, and K. K. Innes, *J. Mol. Spectrosc.*, **33**, 189 (1970); V. A. Job, V. Sethuraman, and K. K. Innes, *ibid.*, **30**, 365 (1969).
(14) V. T. Jones and J. B. Coon, *J. Mol. Spectrosc.*, **31**, 137 (1969).
(15) C. G. Stevens and J. C. D. Brand, *J. Chem. Phys.*, **58**, 3324 (1973); J. C. D. Brand and C. G. Stevens, *ibid.*, **56**, 3331 (1973); J. C. D. Brand and D. S. Liu, *J. Phys. Chem.*, **78**, 2270 (1974).
(16) F. W. Birss, D. A. Ramsay, and S. M. Till, *Chem. Phys. Lett.*, **53**, 14 (1978); D. A. Ramsay and S. M. Till, *Can. J. Phys.*, **57**, 1224 (1979); M. Barnett, D. A. Ramsay, and S. M. Till, *Chem. Phys. Lett.*, **65**, 440 (1979).
(17) D. C. Moule and A. D. Walsh, *Chem. Rev.*, **75**, 67 (1975).
(18) J. H. Clark, C. B. Moore, and N. S. Nogar, *J. Chem. Phys.*, **68**, 1264 (1978).
(19) A. Horowitz and J. G. Calvert, *Int. J. Chem. Kinet.*, **10**, 713 (1978); R. D. McQuigg and J. G. Calvert, *J. Am. Chem. Soc.*, **91**, 1590 (1969).
(20) J. Marling, *J. Chem. Phys.*, **66**, 4200 (1977).
(21) R. S. Lewis, K. Y. Tang, and E. K. C. Lee, *J. Chem. Phys.*, **65**, 2910 (1976).
(22) J. P. Reilly, J. H. Clark, C. B. Moore, and G. C. Pimentel, *J. Chem. Phys.*, **69**, 4381 (1978).
(23) A. C. Luntz and V. T. Maxson, *Chem. Phys. Lett.*, **26**, 553 (1974).
(24) R. G. Miller and E. K. C. Lee, *Chem. Phys. Lett.*, **27**, 475 (1974).
(25) K. Y. Tang, P. W. Fairchild, and E. K. C. Lee, *J. Chem. Phys.*, **66**, 3303 (1977).
(26) J. R. Sodeau and E. K. C. Lee, *Chem. Phys. Lett.*, **57**, 71 (1978).
(27) E. S. Yeung and C. B. Moore, *J. Chem. Phys.*, **58**, 3988 (1973).
(28) E. S. Yeung and C. B. Moore, *J. Chem. Phys.*, **60**, 2139 (1974).
(29) P. L. Houston and C. B. Moore, *J. Chem. Phys.*, **65**, 757 (1976).
(30) J. C. Weisshaar, A. P. Baronavski, A. Cabello, and C. B. Moore, *J. Chem. Phys.*, **69**, 4720 (1978).
(31) J. C. Weisshaar and C. B. Moore, *J. Chem. Phys.*, in press.
(32) R. G. Miller and E. K. C. Lee, *Chem. Phys. Lett.*, **41**, 52 (1976).
(33) R. G. Miller and E. K. C. Lee, *Chem. Phys. Lett.*, **33**, 104 (1975).
(34) R. G. Miller and E. K. C. Lee, *J. Chem. Phys.*, **66**, 4448 (1978).
(35) K. Shibuya and E. K. C. Lee, *J. Chem. Phys.*, **69**, 5558 (1978).
(36) H. L. Selzle and E. W. Schlag, *Chem. Phys.*, in press.
(37) A. C. Luntz, *J. Chem. Phys.*, **69**, 3436 (1978).
(38) J. Troe, work presented at the International Seminar on Photodissociation: Formaldehyde and Beyond, Dec 2-4, 1979, Veldhoven, Holland.
(39) D. F. Heller, M. L. Elert, and W. M. Gelbart, *J. Chem. Phys.*, **69**, 4061 (1978).
(40) M. L. Elert, Ph.D. Dissertation, University of California, Berkeley, 1977.
(41) J. M. F. van Dijk, M. J. H. Kemper, J. H. M. Kerp, H. M. Buck, and G. J. Visser, *Chem. Phys. Lett.*, **54**, 353 (1978).
(42) J. M. F. van Dijk, Ph.D. Dissertation, Eindhoven University of Technology, Eindhoven, 1977.
(43) R. Walsh and S. W. Benson, *J. Am. Chem. Soc.*, **88**, 4570 (1966).
(44) K. Tagaki and T. Oka, *J. Phys. Soc. Jpn.*, **16**, 1174 (1963).
(45) E. K. C. Lee, and G. L. Loper in "Radiationless Transitions", S. H. Lin, Ed., Academic Press, NY, in press.
(46) K. Shibuya, R. A. Harger, and E. K. C. Lee, *J. Chem. Phys.*, **69**, 751 (1978).
(47) M. Zughul, Ph.D. Dissertation, University of California, Berkeley, 1978.
(48) M. Bixon, J. Jortner, and Y. Dothan, *Mol. Phys.*, **17**, 109 (1969).
(49) J. L. Duncan and P. D. Mallinson, *Chem. Phys. Lett.*, **23**, 597 (1973).
(50) W. M. Gelbart, D. F. Heller, and M. L. Elert, *Chem. Phys.*, **7**, 116 (1975).
(51) See K. F. Freed and S. H. Lin, *Chem. Phys.*, **11**, 409 (1975), and references contained therein, for a critical discussion of the use Condon-like approximations in calculating radiationless transition rates.
(52) See, for example, the earlier review article in this journal by P. Avouris, W. M. Gelbart, and M. A. El-Sayed, *Chem. Rev.*, **77**, 793 (1977).
(53) W. H. Miller, *J. Am. Chem. Soc.*, in press.
(54) E. Pollak and P. Pechukas, *J. Chem. Phys.*, **69**, 1218 (1978). We are grateful to Dr. R. Wetmore for reminding us of the possible relevance of the trapped trajectory phenomenon.
(55) See the recent review by B. R. Henry, *Acc. Chem. Res.*, **10**, 207 (1977).
(56) M. J. H. Kemper, J. M. F. van Dijk, and H. M. Buck, *J. Am. Chem. Soc.*, **100**, 7841 (1978).
(57) M. J. H. Kemper, work presented at the International Seminar on Photodissociation: Formaldehyde and Beyond, Dec 2–4, 1979, Veldhoven, Holland.
(58) J. C. Weisshaar and C. B. Moore, work presented at the International Seminar on Photodissociation: Formaldehyde and Beyond, Dec 2–4, 1979, Veldhoven, Holland. See also J. C. Weisshaar, Ph.D. Dissertation, University of California, Berkeley, 1979.
(59) A. Nitzan, J. Jortner, and P. M. Rentzepis, *Proc. R. Soc. London, Ser. A*, **327**, 367 (1972); A. Nitzan and J. Jortner, *Theor. Chim. Acta*, **29**, 97 (1973).
(60) See F. A. Novak, S. A. Rice, and K. F. Freed in "Radiationless Transitions", S. H. Lin, Ed., in press, for a most recent discussion of the influence of rotation on nonradiative electronic relaxation in polyatomic molecules.
(61) W. E. Howard and E. W. Schlag, *J. Chem. Phys.*, **66**, 2679 (1978); *Chem. Phys.*, **29**, 1 (1978).
(62) P. C. Haarhoff, *Mol. Phys.*, **7**, 101 (1963).
(63) K. Sorbie and J. N. Murrell, *Mol. Phys.*, **29**, 1387 (1975).
(64) J. N. Murrell and J. A. Pople, *Proc. Phys. Soc. London, Ser. A*, **69**, 245 (1956).
(65) J. L. Duncan and P. D. Mallinson, *Chem. Phys. Lett.*, **23**, 597 (1973).
(66) E. Hutchisson, *Phys. Rev.*, **36**, 410 (1930); **37**, 45 (1931).
(67) E. Yeung, *J. Mol. Spectrosc.*, **45**, 142 (1973).